

70p.

NASA Contractor Report 172355

Design and Fabrication of the NASA Decoupler Pylon for the F-16 Aircraft, Addendum I

J. D. Clayton and R. L. Haller

GENERAL DYNAMICS

Fort Worth Division

Fort Worth, Texas 76101

Contract NAS1 — 16879
January 1985

(NASA-CR-172355) DESIGN AND FABRICATION OF
THE NASA DECOUPLER PYLON FOR THE F-16
AIRCRAFT, ADDENDUM I Final Report, Aug. -
Oct. 1983 (General Dynamics Corp.) 70 p

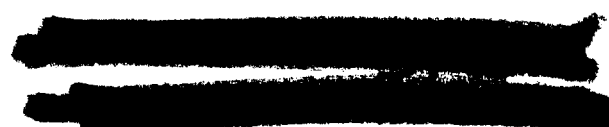
N87-10860

Unclas
CSCL 01C G3/05 43846



National Aeronautics and
Space Administration

Langley Research Center
Hampton, Virginia 23665



NASA Contractor Report 172355

**Design and Fabrication of the
NASA Decoupler Pylon for the
F-16 Aircraft, Addendum I**

J. D. Clayton and R. L. Haller

GENERAL DYNAMICS

Fort Worth Division

Fort Worth, Texas 76101

**Contract NAS1 — 16879
January 1985**



National Aeronautics and
Space Administration

Langley Research Center
Hampton, Virginia 23665



TABLE OF CONTENTS

	PAGE
SUMMARY	1
INTRODUCTION	2
DYNAMIC ANALYSIS, GBU-8 CONFIGURATION	4
Natural Modes of Vibration	4
Flutter Analyses	6
Aeroservoelastic Analyses	9
DYNAMIC ANALYSIS, B-61 CONFIGURATION	11
Natural Modes of Vibration	11
Flutter Analyses	13
Aeroservoelastic Analyses	16
Response to Abrupt Maneuvers	17
MODEL GROUND VIBRATION TESTS - B-61	20
WIND TUNNEL FLUTTER MODEL TESTS - B-61, GBU-8	22
CONCLUSIONS	26
RECOMMENDATIONS	29
REFERENCES	30
TABLES	31
FIGURES	42
APPENDIX A - Symmetric Modes for B-61 on Decoupler Pylon	52
APPENDIX B - Antisymmetric Modes for B-61 on Decoupler Pylon	55
APPENDIX C - Model Ground Vibration Test Modes	58

SUMMARY

The assembled ship set of decoupler pylons was ground tested in a fixture at the General Dynamics, Fort Worth Facility. The results of these ground tests were incorporated into the finite element simulation. The results of flutter analyses and aeroservoelastic analyses performed with the updated model are reported herein. The analyses show that the decoupler pylon will suppress wing-store flutter for the GBU-8 flight test stores configuration on an F-16 airplane.

The feasibility of carrying the B-61 weapon on the decoupler pylon was also evaluated. The pylon design criteria considered only GBU-8 carriage and a series of additional analyses were conducted to evaluate the potential of this pylon for carrying the B-61 weapon without modifications. This series of analyses is reported herein. The analyses show that the pylons would need to be modified in order to demonstrate flutter suppression.

Model ground vibration tests and wind tunnel flutter model tests were conducted to support the anticipated full scale airplane flight test program. The results of the ground vibration tests performed on the 1/4 scale F-16 flutter model and the wind tunnel tests with this model and a model decoupler pylon are reported herein.

INTRODUCTION

The NASA Langley Research Center has investigated the use of a decoupler pylon as a means of suppressing wing/store flutter (References 1 through 6). The concept consists of reducing the pylon pitch stiffness until the store/pylon pitch frequency is less than the fundamental wing bending frequency. These studies and wind tunnel tests have been expanded to include the fabrication of a ship set of pylons for the F-16. These pylons will be used to demonstrate the capabilities of the concept with a flight test program. The pylons are designed to replace the F-16 production weapon pylons which are carried at Stations 3 and 7 (Span Station 120). The details of the decoupler pylon design and the supporting analysis are described in Reference 7 to which this document is an addendum.

The pylons have a beam pitch spring which has a spring rate which was set to increase the airplane flutter speed by the maximum amount for one external store configuration. The external store configuration is identified as GBU-8 configuration and has an AIM-9 and launcher on the wing tips (Stations 1 and 9), the GBU-8 at Stations 3 and 7 (Span Station 120), and 1/2 full 370 gallon tanks at Stations 4 and 6 (Span Station 71). The 370 gallon tanks are loaded with the center bay empty and the forward and aft bays full. The decoupler pylon is designed, from a strength standpoint, to carry all store loadings which are currently carried on Stations 3, 4, 6 and 7.

This addendum to the basic report summarizes the final analyses, which were based upon the results of the ground tests, and reports the results of analyses and tests which were conducted to evaluate the carriage of a second external store on the decoupler pylon. The additional analyses based upon the ground tests included flutter analyses and

aeroservoelastic analyses of GBU-8 configuration. The second store configuration which was evaluated has an AIM-9 launcher at the wing tips (Stations 1 and 9) and the B-61 weapon at Stations 3 and 7. This store configuration is identified as the B-61 store configuration. This store configuration experiences a limited amplitude flutter condition on the F-16 over a range of flight conditions. In 1-g flight the airplane can fly its entire flight envelope without the flutter oscillation amplitude level exceeding a safe level. In high g maneuvers the flutter oscillation amplitude increases to a level which is not considered safe.

DYNAMIC ANALYSIS, GBU-8 CONFIGURATION

The details of the ground tests conducted on the assembled pylon and its components are presented in the basic document (Reference 7). These pylon test results were used to modify the complete airplane finite element simulation. This revised simulation was then used to compute complete airplane modes of vibration and new flutter speeds and to determine flight control system stability.

Natural Modes of Vibration

The initial step in obtaining a tuned complete airplane simulation was to modify the pylon simulation and compare computed influence coefficients and modes of the cantilevered pylon - store with the test data obtained for a rigid support fixture. The pylon simulation was adjusted and readjusted until the comparison between the simulation and the test data was considered acceptable. A comparison between the measured influence coefficients and the final tuned finite element simulation is shown on Table 1. Major modifications were made in the pylon lateral and yaw stiffness of the simulation to improve the correlation between the computed mode shapes and the test data. This modified pylon model correlates with both the influence coefficients which were measured and with the mode shapes and frequencies which were measured. No change was required in the design pylon pitch stiffness to force agreement between the simulation and the test data. The natural frequencies and mode shapes were computed using the tuned cantilevered simulation. These computed frequencies are compared with the measured values on Table 2.

The measured data presented in Tables 1 and 2 reflect the measurements made with the tight fit link pins. After these measurements were made, the pylon pivot pins were

reworked to reduce the frictional breakout forces in the linkage. This rework resulted in free-play in the linkage pins. This free-play effectively creates a nonlinear structure. The nonlinear spring rate results in changes in the natural frequencies as a function of the excitation force. These nonlinear effects were not included in the modal calculations.

The tuned pylon finite element simulation was incorporated into the complete airplane simulation and this revised simulation was used to compute symmetric and antisymmetric modes of vibration. The complete airplane symmetric mode frequencies are shown on Table 3. These frequencies are identified as "tuned decoupler pylon" on Table 3. The first three mode shapes for this case are shown in Reference 7. These computed mode frequencies with the tuned pylon are compared with the production pylon computed frequencies and the decoupler pylon with the preliminary lateral and yaw stiffness and a zero pitch spring. The decoupler pylon with a lateral spring rate which is lower results in a low frequency lateral mode which did not exist on the production pylon or on the preliminary decoupler simulation.

The tuned pylon simulation was also used to compute complete airplane antisymmetric natural frequencies and modes of vibration. These frequencies are identified as "tuned decoupler pylon" on Table 4. The first three mode shapes for this case are shown in Reference 7. These computed mode frequencies with the tuned pylon are compared with the decoupler pylon with zero pitch spring, the decoupler pylon with preliminary stiffness and the production pylon. The decoupler pylon with a lateral spring rate which is lower results in a low frequency lateral mode which did not exist in the preliminary analysis simulation. Natural frequencies and mode shapes have also been computed with a zero pylon

pitch stiffness. These modes and frequencies were used to conduct the open loop spring analysis to evaluate the flutter speeds versus decoupler spring rate.

Flutter Analyses

Flutter analyses which used the modes of vibration described in the previous section were conducted. Two types of analyses were conducted (1) linear pylon spring coupling analyses to determine the flutter velocity as a function of pylon spring rate and (2) nonlinear analyses to determine the linkage frictional effect upon the flutter velocity. The symmetric analyses resulted in high flutter speeds for a wide range of pylon spring rates and therefore the nonlinear type of analyses were restricted to the antisymmetric case only.

The doublet lattice procedure was used to compute the unsteady aerodynamic terms at a Mach number of 0.9. The aerodynamic terms were computed for the antisymmetric modes of vibration with the zero stiffness pylon pitch spring and the other pylon stiffness values tuned to the test data. The generalized masses, generalized stiffness, and the aerodynamic terms were assembled into an open loop problem which can be used to compute the flutter velocity as a function of the pylon spring rate. This type of analysis is conducted by determining the open loop gain at a fixed velocity, and this gain value is converted to spring rate. This type of analysis procedure is described in detail in Reference 7. The spring rate is determined for a set of velocities and a spring rate versus flutter velocity is developed. This curve is shown on Figure 1. The antisymmetric modes result in two unstable roots at spring rate values below 6129 N/cm (3500 lb/in.). The two flutter frequency ranges are from 4.5 to 4.8 Hz and from 5.1 to 5.3 Hz. The instability at both frequencies involves coupling between the lowest four mode shapes. Both flutter roots have

high flutter speeds in the spring rate range of 3502 N/cm (2000 lb/in.), which is the spring rate value in the actual hardware.

The ground vibration tests of the decoupler pylon on the fixture revealed a high friction level in the linkage pins. At low excitation force levels the pylon pitch frequency was 5.5 Hz. This mode is an upper strongback bending between the two wing/pylon attachment points. This upper strongback bending results in GBU-8 pitch motion. At high force levels the primary store pitch mode is excited. This mode has a frequency of 3.6 Hz. Breakout tests and changes in the linkage pins revealed the source of the friction which is in the pivot pin bushings. The pylon system with a frequency which changes as a function of excitation force is nonlinear and therefore a nonlinear flutter analysis was conducted.

The nonlinear analysis was conducted with two pitch spring rates, (1) the stiff spring rate at a low force level and (2) the soft spring rate at a higher force level. There were inadequate measurements made during the influence coefficient tests to determine the pitch spring rate at the low amplitude. To determine the low amplitude pitch spring rate, the pitch frequency ratio was used. The spring rate ratio is related to the frequencies by the following equation:

$$\frac{k_{\theta_1}}{k_{\theta_2}} = \left(\frac{5.5}{3.6} \right)^2$$

where k_{θ_1} is the spring rate below breakout, which is unknown and k_{θ_2} is the design spring rate which is 3502 N/cm (2000 lb/in.) acting 111.76 cm (44 in.) from the store C.G. The rotation spring rate is:

$$k_{\theta_2} = (3502)(111.76)^2 = 4.374 \times 10^7 \text{ N cm/rad} \\ (3.872 \times 10^6 \text{ in.lb/rad})$$

$$\text{and } k_{\theta_1} = (5.5/3.6)^2 \times 4.374 \times 10^7 = 1.021 \times 10^8 \text{ N cm/rad} \\ (9.037 \times 10^6 \text{ in.lb/rad})$$

which is the spring rate value below the frictional breakout value. The static breakout was measured and is 678 N m (6000 in.lb). This breakout moment and the spring rate below breakout were used to compute the angle at which breakout will occur.

$$6000/(9.037 \times 10^6) = .66393 \times 10^{-3} \text{ rad} = .03804 \text{ deg}$$

In summary the spring rate below ± 0.03804 degrees is 1.021×10^6 N m/rad (9.037×10^6 in.lb/rad) and between ± 0.03804 degrees and ± 3 degrees the spring rate is 4.374×10^5 N m/rad (3.872×10^6 in.lb/rad). The characteristics of this nonlinear spring rate are shown on Figure 2. At ± 3 degrees the pylon contacts the stops and $k_{\theta_1} = 1.021 \times 10^6$ N m/rad (9.037×10^6 in.lb/rad). With this data a nonlinear flutter analysis was conducted. The second ingredient in the analysis is a pitch spring rate versus flutter speed curve. This curve was generated and is shown on Figure 1.

The nonlinear analysis is based on the describing function or equivalent linearization method. This method is described in detail in Reference 3. The basis of the describing function method is to assume a sinusoidal displacement and then compute the load developed in the nonlinear spring. Using these assumptions, a set of nonlinear analyses were conducted. These analyses results are shown on Figure 3. The parameters which are used to describe the results are illustrated in Reference 7, Figure 29, and defined below.

- \bar{M} - Static Preload Moment (oscillations occur about this moment).
- M_0 - Static Moment required to deflect store to breakout value; 678 N m (6000 in.lb).
- θ_1 - Amplitude of store pitch oscillation.
- θ_0 - Pitch Angle at which store breaks friction (0.03804 degrees).
- δ - Describing function ($\delta = K_e/K$) where K_e is the equivalent linear spring constant of the nonlinear spring.

The analysis indicates that there are small changes in the flutter speed as a function of large variations of the ratio \bar{M}/M_0 . This is due to the small angular range over which the pylon is below breakout.

Aeroservoelastic Analyses

Symmetric and antisymmetric aeroservoelastic analyses were conducted using the pylon simulation based on ground test data. Both analyses were made at a Mach number of 0.9 and at an altitude of sea level. The symmetric analysis was conducted with the pitch loop open. At 305 m/s (594 kts) at sea level the pitch loop has a large gain and phase margin. Since the pitch loop margins were large, the analysis was not conducted at additional velocities.

The antisymmetric analysis was conducted with the yaw loop closed and the gain and phase margins were determined from the open loop roll response. The analysis was conducted with the unsteady aerodynamic terms computed for a Mach number of 0.9. The gain and phase margins were determined for a series of velocities. By conducting the analysis with the yaw loop closed, the stability of the yaw loop is

determined by observing the determinant of the right hand side matrix. From the open loop roll response, stability of the roll loop is determined and gain and phase margin is determined. The analyses were initially conducted with a damping of zero in the rigid body degrees of freedom and a damping value of 0.01 in all the flexible degrees of freedom. The results of this analysis are shown on Table 5. The airplane is stable and has sufficient gain and phase margin at speeds up to 271 m/s (528 kts). At 305 m/s (594 kts) the yaw loop drives the airplane unstable and the roll loop does not stabilize the instability. At the lower velocities the yaw loop creates no instability and the roll loop has more than adequate gain and phase margins. At 305 m/s (594 kts), a 90° phase lead in the roll loop and a factor of three increase in the roll loop gain are required to stabilize the instability created by the yaw loop. The flutter analysis reported in the previous section revealed a lowly damped root which crosses zero damping at 283 m/s (550 kts) and reaches a maximum damping value of 0.019 at 418 m/s (813 kts). Therefore the analysis results shown on Table 5 with low damping reflect the flutter instability. The analysis was repeated using a damping value of 0.02 in each flexible mode and at a velocity of 305 m/s (594 kts). The analysis was conducted with the yaw loop closed and the gain and phase margin of the roll loop was determined. These margin values are shown on Table 5. The highest response occurs at a frequency of 5.1 Hz (the flutter mode frequency) which indicates that there is the potential for an instability at this frequency if low damping exists. Since damping values in excess of 0.02 are expected in the airplane structure and in the decoupler pylon, this lowly damped instability is not expected on the airplane.

DYNAMIC ANALYSIS, B-61 CONFIGURATION

A series of analyses were conducted to evaluate the dynamic effects of using the decoupler pylon on the B-61 store configuration. The GBU-8 weapon weighs 10.08kN (2265 lb.) whereas the B-61 weapon weighs 3.336kN (750 lb.). The weapon pitch inertia is also much higher on the GBU-8 weapon. These differences result in a higher store pitch frequency when carrying the B-61. The analysis results of this store change are reported here. The same methods of analysis which were utilized on the GBU-8 configuration and are reported in Reference 7 were used in the analysis of the B-61 store configuration. Three types of analyses were conducted. These are: (1) flutter analyses, (2) aeroservoelastic analyses, and (3) response to abrupt maneuvers.

Natural Modes of Vibration

The symmetric and antisymmetric natural frequencies and modes of vibration of the complete airplane were required to conduct the flutter analysis and the aeroservoelastic analyses. A finite element representation of the airplane structure was employed to compute the modes of vibration. This finite element representation is described in detail in Reference 8. This finite element model was loaded with the B-61 configuration mass and inertia to develop the dynamic matrix which was used to compute modes of vibration. Weapon pylon simulations of both the production pylon and the decoupler pylon were developed and used independently to compute the modes for both cases. The details of these two pylon simulations are described in Reference 8.

The symmetric complete airplane mode frequencies for the production pylon simulation and the decoupler pylon simulation are shown on Table 6. A description of each of the first eight lowest frequency modes is also included on

Table 6. The mode shapes for the three lowest frequency modes with the decoupler pylon are shown in Appendix A. The decoupler pylon has the effect of changing the wing bending frequency from 6.08 Hz to 5.99 Hz. The B-61 store pitch mode frequency is reduced from 9.33 Hz to 6.19 Hz. Also the higher frequency modes are reordered due to the effect of the decoupler pylon. The mode frequencies computed with the decoupler pylon simulation with a zero pitch stiffness spring in the decoupler are also shown on Table 6. Without the pitch spring the B-61 pitch mode is eliminated. The frequencies of the other modes are only altered slightly by removing the decoupler pitch spring. The first three mode shapes with the zero decoupler pitch spring are shown in Appendix A.

The antisymmetric complete airplane mode frequencies for the production pylon simulation and the decoupler pylon simulation are shown on Table 7. A description of each of the first seven lowest frequency modes is also included on Table 7. The mode shapes for the three lowest frequency modes with the decoupler pylon are shown in Appendix B. The decoupler pylon has the effect of changing the wing bending frequency from 10.09 Hz to 9.82 Hz. The B-61 store pitch mode frequency is reduced from 9.043 Hz to 6.11 Hz. This separation of the first two mode frequencies, which is the result of the decoupler, has a significant effect upon the flutter speed. The mode frequencies computed with the decoupler pylon simulation with a zero pitch stiffness spring in the decoupler are shown on Table 7. Without the pitch spring the B-61 pitch mode is eliminated. The frequencies of the other modes are altered slightly by removing the decoupler pitch spring. The first three mode shapes with the decoupler zero pitch spring are shown in Appendix B.

Flutter Analyses

Symmetric and antisymmetric flutter analyses of the B-61 store configuration were conducted with the production pylon simulation and with the decoupler pylon simulation. The analyses were the bases for evaluating the effectiveness of the decoupler pylon as a flutter suppression device on the B-61 store configuration. These analyses were conducted for subsonic Mach numbers of 0.6 and 0.9 and a supersonic Mach number of 1.2. The subsonic unsteady aerodynamic terms were computed with the doublet lattice aerodynamic program and the supersonic unsteady aerodynamic terms were computed with the kernel function procedure.

The initial analyses were made to compare the production pylon and the decoupler pylon with the current design spring. These comparisons were made at an altitude of sea level for the three Mach numbers. A standard k solution flutter analysis was made. The flutter speed and flutter frequencies were compared at a damping value of 0.02. These flutter speeds and flutter frequencies are shown on Table 8. The production pylon analysis shows high flutter speeds for the symmetric cases and low flutter speeds for the antisymmetric cases. These results agree with the airplane flight test experience, where the limited amplitude oscillations are antisymmetric. The flight experience is such that as speed is increased, the magnitude of the oscillation increases, therefore a clear cut flutter instability is experienced on the airplane. The predicted antisymmetric flutter frequency also matches the frequency experienced in flight.

The flutter analysis of the airplane with the decoupler pylon results in a low symmetric and a high antisymmetric flutter speed. Therefore the decoupler pylon has the effect of solving the antisymmetric flutter problem and creating a symmetric flutter problem. The low symmetric flutter speed

is the result of having driven the first two mode frequencies very close together (5.99 Hz and 6.19 Hz). In the antisymmetric case, the decoupler pylon separates the wing bending mode and the store pitch mode frequencies (6.11 Hz and 9.82 Hz). This separation results in an increase in flutter speed.

The flutter analysis of the B-61 configuration with the decoupler pylon and a spring designed for the GBU-8 weapon indicates that a change in spring rate was required on the B-61 configuration. A series of additional analyses were therefore conducted to determine the optimum B-61 spring rate for both the symmetric and antisymmetric cases. A series of pylon spring coupling analyses were conducted to determine the pylon pitch spring rate which would result in an increase in flutter speed for both the symmetric and antisymmetric cases. The method which was used is to treat the decoupler pylon spring as a feedback loop in a feedback mechanism. With this approach it is possible to develop a spring rate versus flutter velocity curve and determine the spring rate at which the maximum flutter speed occurs. This type of analysis requires the set of mode shapes with zero decoupler pylon spring stiffness. These mode shapes and frequencies were computed; the mode shapes are shown in Appendices A and B, and the mode frequencies are shown on Tables 6 and 7. The unsteady aerodynamic terms were computed using these mode shapes and the doublet lattice aerodynamic procedure for a Mach number of 0.9. The open loop frequency response was computed for a series of velocities to determine the pitch spring rate at these velocities.

The results of the symmetric analysis are shown on Figure 4. The spring rate is defined in terms of a linear spring acting 111.76 cm (44 in.) aft of the store center of gravity. The center of gravity is located halfway between the MAU-12 hooks. The lowest flutter speed occurs at a

spring rate of approximately 3502 N/cm (2000 lb/in.), which is the value in the current decoupler design. The results of the v-g solution are also shown on Figure 4 for comparison with the open loop results. The difference in velocity between the v-g solution and the open loop solution is due to small changes in the mode shapes between the finite decoupler spring and the zero spring modes. Structural damping values of 0.02 in the flexible modes were used to predict the flutter velocity in both cases. A softer or a stiffer pitch spring with respect to the current design will result in a higher flutter speed.

The results of the spring coupling analyses of the antisymmetric modes of vibration are shown in Figure 5. The spring rate is defined in terms of a linear spring acting 111.76 cm (44 in.) aft of the store center of gravity. The center of gravity is located halfway between the MAU-12 rack hooks. The lowest flutter speed occurs at the highest spring rate and the flutter speed increases as the spring rate decreases. In the spring rate range from approximately 3502 N/cm (2000 lb./in.) to 10506 N/cm (6000 lb./in.) there is a narrow region of instability and at higher velocities the flutter condition would again become stable. The phenomenon is analogous to a velocity damping solution which crosses zero damping as velocity increases and then with further increases in velocity crosses back over zero damping and becomes stable. At the higher spring rates where the higher velocity stable region does not exist, the damping approaches zero without crossing it. At a spring rate of approximately 5255 N/cm (3000 lb./in.). The unstable velocity region is very narrow. The flutter analysis results obtained with spring coupling were compared with the v-g solution approach on Figure 5 for a spring rate of 3502 N/cm (2000 lb./in.). The small difference in flutter speed between the v-g solution and the spring coupling solution is due to small

changes between the mode shapes computed with a finite decoupler spring and the zero spring modes.

Considering both the symmetric results shown on Figure 4 and the antisymmetric results shown on Figure 5, a spring rate of approximately 1751 N/cm (1000 lb/in.) is required to satisfy both flutter requirements.

Aeroservoelastic Analyses

A series of analyses were conducted to determine the stability of the B-61 store configuration with the flight control system engaged. The gain and phase margins were determined for the pitch channel in the symmetric case for both the production pylon and the decoupler pylon. In the antisymmetric case the gain and phase margins for the roll channel were determined with the yaw loop closed for both the production pylon and the decoupler pylon. The analyses used the unsteady aerodynamic data computed by the doublet lattice aerodynamic procedure for Mach numbers of 0.6 and 0.9. The analysis was conducted at an altitude of sea level and at velocities of 204 m/s (397 kts) and 305 m/s (594 kts) which are Mach numbers of 0.6 and 0.9. Aeroservoelastic analyses of the F-16 airplane with other external store configurations have shown that minimum flight control system gain and phase margins occur at high transonic speeds at low altitude. Therefore the flight conditions described were chosen for the analysis. The flight control system gains for these flight conditions were used in the stability margin evaluations.

The symmetric analysis of the open loop pitch channel response with the production pylon indicates that it has an adequate gain and phase margin for the analysis conditions described above. The flutter analysis of the B-61 configuration indicates that the existing decoupler spring rate of 3502 N/cm (2000 lb/in.) results in a symmetric

flutter speed which is below the aeroservoelastic analysis speed. A symmetric analysis was conducted with the 3502 N/cm (2000 lb/in.) decoupler spring to determine if the flight control system pitch channel would stabilize this flutter instability. This analysis indicated that the pitch channel did not provide stability for the flutter instability. Therefore the symmetric analysis of the decoupler pylon case was repeated with a 1751 N/cm (1000 lb/in.) spring rate. Since a 1751 N/cm (1000 lb/in.) spring is required for the symmetric case an antisymmetric analysis was also conducted with this spring rate.

The results of the symmetric analysis with a 1751 N/cm (1000 lb/in.) spring rate in the decoupler pylon indicate that the airplane with the pitch loop is stable with large gain and phase margins at velocities of 204 m/s (397 kts) and 305 m/s (594 kts). The results of the antisymmetric analysis with a 1751 N/cm (1000 lb/in.) spring rate in the decoupler pylon are summarized on Table 9. These stability margins were obtained from the open loop roll channel response with the yaw loop closed. The closed loop yaw channel has large stability margins at both velocities. The conclusion from these analyses is that the B-61 configuration with the decoupler pylon with a 1751 N/cm (1000 lb/in.) pitch spring will be stable throughout the entire operational envelope of the store configuration.

Response to Abrupt Maneuvers

The speed and maneuver envelope for the B-61 configuration considered in determining maximum store pitch moment included all speeds from 0 to 600 KEAS or 1.2 Mach number, whichever is less. This analysis used altitudes from sea level to 20,000 feet and assumed that altitudes above this are noncritical. Aircraft maneuvers which were reviewed included -2.0g and 5.5g symmetric maneuvers, -1.0g, 1.0g and

4.4g roll maneuvers with maximum bank angle change of 180° , and 1.0g sideslip maneuvers ranging from maximum positive sideslip angles to maximum negative sideslip angles. The six components of load for each of the maneuvers at 14 Mach/altitude points were computed. These load conditions were searched for maximum and minimum store only pitch moment.

Those maneuvers which produce large B-61 store pitching moments during dynamic conditions were selected. These conditions are:

<u>Mach</u>	<u>Altitude</u>	<u>Maneuver Type</u>
0.95	2500	-2g Abrupt Push-Over
0.90	S.L.	-1g 180° Roll
0.95	2500	4.4g 180° Roll

The response time histories were computed for these load conditions. The maximum store-only pitching moments during these maneuvers are:

<u>Mach</u>	<u>Altitude</u>	<u>Store-Only Pitching Moment</u> N m (In.Lb.)	
		<u>Left Wing</u>	<u>Right Wing</u>
0.95	2500	-2950(-26113)	-2954(-26144)
0.90	S.L.	-2941(-26031)	-2217(-19628)
0.95	2500	3807(33699)	-1330(-11775)

The store only loads are referenced to the store c.g. location which is fuselage station 338.4 and water line 68.3. The load time histories of the store loads were applied to the store and decoupler pylon system to compute pylon alignment time histories. The time history response analysis

of the decoupler alignment system was conducted for the 4.4g roll maneuver. The analysis was conducted for decoupler spring rates of 3502 N/cm (2000 lb/in.) and 1751 N/cm (1000 lb/in.). The time history response for the decoupler pylon with a 3502 N/cm (2000 lb/in.) spring is shown on Figure 6. The analysis was conducted with the alignment motor off and repeated with the alignment motor on. The case with the motor on has the switches set to come on at a misalignment of $\pm 0.5^\circ$ and to turn off at $\pm 0.25^\circ$. The maximum misalignment angle with the alignment motor inactive is 0.7° . The maximum misalignment angle with the alignment motor active is -0.67° which is no significant improvement.

The time history response for the decoupler pylon with a 1751 N/cm (1000 lb/in.) spring is shown on Figure 7. The analysis was conducted with the alignment motor off and repeated with the alignment motor on. The case with the motor on has the switches set to come on at $\pm 0.5^\circ$ and turn off at ± 0.25 degrees. The maximum misalignment angle with the alignment motor inactive is 1.48° . The maximum misalignment angle with the alignment motor active is -1.26° .

These analyses indicate that the alignment system in its current configuration will operate satisfactorily on the B-61 configuration. The alignment system is not, however, as effective as it is on the GBU-8 weapon.

MODEL GROUND VIBRATION TESTS - B-61

Ground vibration tests of the 1/4 scale F-16 flutter model were conducted. The purpose of these tests was to determine the natural frequencies and mode shapes of the B-61 store configuration with the production pylons. The store configuration has been wind tunnel tested on two previous occasions. The flutter model has two sets of wings. The original model wings have been used extensively for stores clearance. These wings have flaperons which are held with cloth hinges and the actuator stiffness is simulated with a leaf spring. A second set of model wings was fabricated in 1978. These wings are dynamically the same as the original wings, with hinged flaperons that are actuated with actuators at the root of the flaperons. These wings are identified as the flutter suppression wings. The first wind tunnel test of the B-61 configuration was conducted with the original model wings. During these tests flutter was encountered. The second wind tunnel test of the B-61 configuration was conducted on the flutter suppression wings. This test was conducted to dynamic pressures much above the test conditions of the first test without encountering flutter.

These ground vibration tests of the model were conducted to determine if differences between the two sets of model wings could be detected which would explain the difference in the wind tunnel test results. Earlier static deflection tests of the two sets of wings revealed no difference. Therefore, the lowest frequency modes were measured with both sets of wings. The measured natural frequencies are shown on Table 10 for both wing configurations. The lowest four mode shapes for each wing configuration are shown in Appendix C. With the exception of the B-61 yaw mode, the frequencies are very close to the same for both sets of wings. The B-61 yaw mode frequency is different between the two wings and also different between the left hand and right hand side. Since

the stores and pylons are the same for the tests of both wing sets, these yaw mode differences are attributed to small differences in the pylon attachment stiffness in each of the four wings. The smaller differences in the B-61 pitch frequencies indicate that the pitch support stiffness is more uniform between left and right and the two sets of wings.

The flutter mode is primarily a coupling between the wing bending mode and the B-61 pitch mode. The small difference in the frequencies and mode shapes which were measured does not appear to be significant enough to change the flutter characteristics between the two wing sets.

WIND TUNNEL FLUTTER MODEL TESTS - B-61, GBU-8

Wind tunnel flutter model tests were conducted in the NASA Langley 16 foot Transonic Dynamics Tunnel to demonstrate the effectiveness of the decoupler pylon to suppress wing/store flutter. All tests conducted prior to the tests reported here used a decoupler pylon which had a single pivot. One of the conclusions from these earlier tests was that maximum increase in flutter speed was obtained with a decoupler design which has its pivot location as close to the wing plane as possible. The disadvantage of this pylon configuration is that during maneuvers the misalignment angles are larger than when the pivot location is near the store C.G. The airplane hardware which will be flight tested has a remote pivot which coincides with the store C.G. The purpose of wind tunnel tests reported here was to demonstrate that the remote pivot decoupler pylon design was as effective in suppressing flutter as the single pivot design had demonstrated in earlier wind tunnel tests. A second objective was to demonstrate that the friction which exists in the full scale hardware pins, did not adversely effect the flutter suppression characteristics of the pylon. The wind tunnel demonstrations of the remote pivot design were started on August 1, 1983 and were completed on August 5, 1983.

A ship set of decoupler pylons which were geometrically scaled models of the full scale article was designed and fabricated by Dynamic Engineering Inc. The internal arrangement of the pylon is shown in Figure 8. The model pylons had a scaled stiffness beam spring and an air damper. Active pitch alignment was not provided. A threaded screw was provided and alignment position could be set and locked for each run. The pylon with the nose, trailing edge and one

side fairing installed is shown on Figure 9. The pylon with the model GBU-8 weapon installed is shown on Figure 10.

The 5 days of tunnel testing are summarized on Table 11. Two external store configurations were tested. The GBU-8 configuration was tested with both the production weapons pylon and the decoupler pylon. The configuration was tested with two external fuel tank loadings. The decoupler pylon tests were conducted with no friction and two levels of increased friction. The B-61 configuration was the second store configuration tested and it was tested with the production pylon only.

The B-61 external store configuration with the production pylon had encountered flutter when tested earlier on the original model wings but not when tested on the flutter suppression wings. Unfortunately the original model wings were destroyed by flutter during tests of another configuration and were not available for these tests. The flutter points could not be repeated with the flutter suppression wings, even though there is no indication from ground tests that the two sets of wings were different. The test was terminated because with no flutter points the decoupler pylon test would have no purpose.

The decoupler pylons were modified to incorporate friction into the system. A spring loaded bolt was added which pulled the pylon fairing into pads which were bonded to the lower portion of the pylon. The tension in the bolt could be increased or decreased to change the pressure between the side panels of the fairings and the balsa pads bonded to the lower portion of the pylon. Ground tests of the full scale pylons have shown that a moment of 678 N m (6000 in. lb) was required to breakout the friction (ref. 7). The breakout friction level was simulated on the model pylons. The scaling factor on moment between airplane and

model is 429.64. The airplane to model scaling factors are shown in Reference 9. The moment on the model is:

$$\frac{678}{429.6} = 1.578 \text{ N m (13.96 in.lb)}$$

The decoupler pylons were mounted in a fixture to apply this moment. A plate was bolted to the bottom of the pylons which had a load application point which was 26.03 cm (10.25 inches) forward of the linkage apex. The load required at this point is:

$$\frac{1.578}{.2603} = 6.06 \text{ N (1.36 lbs)}$$

The tension spring was set and locked so that at 4.448 N (1 lb) of load breakout did not occur and at 6.09 N (1.37 lbs) breakout occurred. The breakout status was obtained by monitoring the spring strain gage. Both pylons were set with this same level of breakout friction.

After completing Run No. 39 (Table 11), the decoupler pylons were removed from the model and the breakout friction was checked. The friction was the same as before Run No. 38. The friction was increased to a level which was twice the level tested on runs 38 and 39. This increased friction was accomplished by increasing the tension in the bolts in the pylon fairing. The tension was increased until the breakout would not occur at 8.896 N (2 lbs) of load at 26.03 cm (10.25 inches) from the pylon apex, and would breakout at 12.23 N (2.75 lbs). Both pylons were set and locked using this criteria.

After completing Run No. 41 (Table 11), the decoupler pylons were removed from the model and the breakout friction was checked on pylon No. 2 (right hand side). The pylon would not breakout with 6.672 N (1.5 lbs) of weight and would breakout with 7.784 N (1.75 lbs). This test indicated that the friction which was in the pylons at the beginning of run No. 41 had been reduced during the run. There was an indication that the friction surfaces were more polished than before the run.

The conclusions which were obtained from the five days of wind tunnel tests are that the decoupler pylon with a remote pivot is just as effective in increasing the wing/store flutter speed as the single pivot pylon design is. Also, increased friction in the pylon pivot to levels comparable to the full scale hardware, does not effect the capability of the pylon for increasing the flutter speed.

CONCLUSIONS

A ship set of decoupler pylons was designed, analyzed and fabricated for a flight test evaluation. The pylons were designed for GBU-8 carriage and the analyses and tests described here were conducted to complete the evaluation of the GBU-8 carriage and to evaluate the potential of these pylons for carriage of the B-61 weapon.

A final analysis of the airplane with the GBU-8 configuration was conducted. This analysis was based upon using a complete airplane model which was tuned to match the pylon ground test results. The flutter analysis using this model indicated that the decoupler pylon was equally as effective as was indicated by the preliminary analyses. A nonlinear flutter analysis which included the linkage friction which was measured during the ground tests was conducted. This analysis indicated that the pylon will break out of the friction at small angles and the friction will have no detrimental effect upon the flutter characteristics.

Wind tunnel tests of the flutter model have been conducted on the B-61 configuration on two previous occasions. The first of these tests was conducted with the original model wings. In this test flutter was encountered. The second of these tests was conducted on the model with the flutter suppression wings. In this test flutter was not encountered. Ground vibration tests of the model were conducted with both sets of wings to determine if differences between the two sets of wings could be detected. These test results indicated very small differences between the two sets of wings. These small differences do not appear to be large enough to explain the difference obtained during the two wind tunnel tests of the configuration.

In order to evaluate the effectiveness of the remote pivot design decoupler pylon, a wind tunnel model flutter test was conducted. These tests indicated that the remote pivot design was equally as effective in suppressing flutter as the single pivot design. The effect of friction was also evaluated on the wind tunnel model, and there was no adverse effect of friction in the pylon linkage.

The current design decoupler pylons with a 3502 N/cm (2000 lb/in.) spring rate, which is optimum for the GBU-8 weapon carriage, were evaluated for carrying the B-61 weapon. The B-61 is much lighter than the GBU-8. The weapon pitch inertia is also much less. Flutter analyses, aeroservoelastic analyses, and response to abrupt maneuvers were conducted on the airplane with the B-61 configuration. The flutter analysis indicated that the decoupler pylon increased the airplane antisymmetric flutter speed by a large amount. The analysis also indicated that the symmetric flutter speed was reduced to an unacceptable level by the decoupler pylon. Variations of the decoupler spring rate were made to determine a spring rate which would increase this symmetric flutter speed while not decreasing the antisymmetric flutter speed. The decoupler spring rate which met these requirements has a value of 1751 N/cm (1000 lb/in.).

Aeroservoelastic analyses of the B-61 configuration with the decoupler pylon with a 1751 N/cm (1000 lb/in.) and a 3502 N/cm (2000 lb/in.) spring rate were conducted. These analyses indicated that the flight control system gain and phase margins were adequate with both spring rates.

An abrupt maneuver analysis was conducted on the B-61 configuration with the 1751 N/cm (1000 lb/in.) spring rate. Maneuver conditions which create large store only pitch moments were selected for evaluation on the decoupler pylon.

These analyses indicated that the current configuration of the alignment system and the current alignment system switching arrangement were adequate for the pylon with the B-61 weapon (but not as effective as for the GBU-8 configuration).

RECOMMENDATIONS

It is recommended that a flight test demonstration of the decoupler pylon on the F-16 be performed. The initial test should be performed on GBU-8 configuration which has experienced limited amplitude flutter inside the airplane operation limit. After completing the tests of GBU-8 configuration the pylon should be retrofitted with a set of 1751 N/cm (1000 lb/in.) springs and a second flight test demonstration performed on the B-61 configuration. This second test will show the effectiveness of the decoupler pylon in suppressing flutter on the B-61 configuration. The flight test program should include high g maneuvers at high dynamic pressures to demonstrate the ability of the decoupler pylon to suppress the flutter condition which increases in amplitude as a function of the maneuver load.

REFERENCES

1. Reed, Wilmer H., III; Foughner, Jerome T., Jr.; and Runyan, Harry L.; Decoupler Pylon: A Simple Effective Wing/Store Flutter Suppressor AIAA J. Aircraft, Vol. 17, No. 3, March 1980, pp. 206-211.
2. Runyan, Harry L.; Effect of a Flexibly Mounted Store on the Flutter Speed of a Wing, NASA CR-159245, April 1980.
3. Desmarais, Robert N.; and Reed, Wilmer H., III; Wing/Store Flutter With Nonlinear Pylon Stiffness, AIAA J. Aircraft, Vol. 18, No. 11, November 1981, pp. 984-987.
4. Reed, Wilmer H., III; Cazier, Frank W., Jr.; and Foughner, Jerome T., Jr.; Passive Control of Wing/Store Flutter, Presented at the Fifth JTGG/MD Aircraft Stores Compatibility Symposium in St. Louis, Mo., September 1980.
5. Cazier, F. W., Jr.; and Foughner, Jerome T., Jr.; NASA Decoupler Pylon Programs for Wing/Store Flutter Suppression, NASA CP-2162, Part 1, Vol. 1, pp. 207-218.
6. Reed, Wilmer H., III; Cazier, F. W., Jr.; and Foughner, Jerome T., Jr.; Passive Control of Wing/Store Flutter, NASA TM-81865, December 1980.
7. Clayton, J. D.; Haller, R. L.; and Hassler, J. M., Jr.; Design and Fabrication of the NASA Decoupler Pylon for the F-16 Aircraft, NASA CR-172354, January 1985.
8. Peloubet, R.P., Jr.; Haller, R.L.; and McQuien, L.J.; Feasibility Study and Conceptual Design for Application of NASA Decoupler Pylon to the F-16, NASA CR-165834, May 1982.
9. Peloubet, R.P., Jr.; Haller, R. L.; Wind Tunnel Demonstration of an Active Flutter Suppression System Using F-16 Model with Stores, AFWAL-TR-83-3046, Vol. I, April 1983.

TABLE 1.- DECOUPLER PYLON INFLUENCE COEFFICIENTS
FOR CANTILEVERED PYLON AND GBU-8 STORE

LOAD DIRECTION	DEFLECTION DIRECTION	*INFLUENCE COEFFICIENT (DEFLECTION PER UNIT LOAD)		
		GROUND TEST		FINITE ELEMENT
VERTICAL	VERTICAL	8.51 x 10 ⁻⁶	(1.49 x 10 ⁻⁵)	8.39 x 10 ⁻⁶
	SIDE	1.34 x 10 ⁻⁶	(2.35 x 10 ⁻⁶)	**
	PITCH	5.99 x 10 ⁻⁸	(2.66 x 10 ⁻⁷)	9.41 x 10 ⁻⁸
	ROLL	7.25 x 10 ⁻⁸	(3.22 x 10 ⁻⁷)	**
SIDE	YAW	1.65 x 10 ⁻⁸	(7.35 x 10 ⁻⁸)	**
	SIDE	5.89 x 10 ⁻⁵	(1.031 x 10 ⁻⁴)	5.68 x 10 ⁻⁵
	PITCH	7.50 x 10 ⁻⁸	(3.332 x 10 ⁻⁷)	**
	ROLL	1.36 x 10 ⁻⁶	(6.056 x 10 ⁻⁶)	**
PITCH	YAW	2.10 x 10 ⁻⁷	(9.335 x 10 ⁻⁷)	1.34 x 10 ⁻⁶
	PITCH	2.24 x 10 ⁻⁸	(2.53 x 10 ⁻⁷)	2.10 x 10 ⁻⁷
	ROLL	9.89 x 10 ⁻¹⁰	(1.118 x 10 ⁻⁸)	2.48 x 10 ⁻⁸
	YAW	3.85 x 10 ⁻¹⁰	(4.354 x 10 ⁻⁹)	**
ROLL	ROLL	4.15 x 10 ⁻⁸	(4.69 x 10 ⁻⁷)	**
	YAW	9.41 x 10 ⁻¹⁰	(1.063 x 10 ⁻⁸)	4.12 x 10 ⁻⁸
YAW	YAW	1.07 x 10 ⁻⁸	(1.211 x 10 ⁻⁷)	1.12 x 10 ⁻¹²
				1.07 x 10 ⁻⁸
				(4.65 x 10 ⁻⁷)
				(1.265 x 10 ⁻¹¹)
				(1.212 x 10 ⁻⁷)

* ANGULAR DISPLACEMENT UNITS ARE RADIAN, LOADS ARE N(LB),
MOMENTS ARE N m (IN.LB), LINEAR DISPLACEMENTS ARE CM(IN.).

** SIMULATION DOES NOT HAVE THIS COUPLING DEGREE OF FREEDOM.

TABLE 2.- NATURAL FREQUENCIES FOR CANTILEVERED PYLON AND GBU-8 STORE.

MODE	NATURAL FREQUENCY - HZ	
	GROUND TEST	FINITE ELEMENT
FIRST STORE PITCH	3.6	3.667
SECOND STORE PITCH	5.5	5.494
*STORE LATERAL	5.7	5.223
STORE YAW	6.7	6.644

* THERE IS SOME YAW MOTION COUPLED IN THE LATERAL MODE.

TABLE 3.- COMPLETE AIRPLANE PREDICTED SYMMETRIC MODE FREQUENCIES - GBU-8 STORE.

MODE	TUNED DECOUPLER PYLON (HZ)	PRELIMINARY STIFFNESS DECOUPLER PYLON (ZERO PITCH SPRING) (HZ)	PRODUCTION PYLON (HZ)
WING BENDING	3.694	3.881	3.869
GBU-8 PITCH	3.259	-	5.343
GBU-8 LATERAL	5.123	-	-
GBU-8 YAW	5.309	6.556	7.409
TIP MISSILE PITCH	5.955	6.047	6.135
WING TORSION (TIP MISSILE PITCH)	6.603	-	-
TANK PITCH	7.381	6.743	8.014
TANK YAW	7.923	7.882	7.843
WING 2ND BENDING	9.980	8.796	10.774
FUSELAGE VERT. BENDING	11.757	11.986	11.859
TANK YAW	14.175	14.693	14.453

TABLE 4.- COMPLETE AIRPLANE PREDICTED ANTISYMMETRIC MODE FREQUENCIES -
GBU-8 STORE.

MODE DESCRIPTION	TUNED DECOUPLER PYLON (HZ)	TUNED DECOUPLER PYLON (ZERO PITCH SPRING) (HZ)	PRELIMINARY STIFFNESS DECOUPLER PYLON (HZ)	PRODUCTION PYLON (HZ)
GBU-8 PITCH	3.22	4.58	3.44	5.11
GBU-8 LATERAL	4.90			
GBU-8 YAW	5.21	4.95	6.39	7.12
TIP MISSILE PITCH	5.54	5.52	5.42	5.42
GBU-8 YAW	6.20	6.19	8.19	8.36
TANK PITCH	7.11	7.08	6.61	7.88
TANK YAW	7.98	7.98	7.98	7.98
WING BENDING	8.72	8.71	9.85	10.48
VERT. TAIL BENDING	11.74	11.72	11.62	11.99

TABLE 5.- LATERAL AIRPLANE AEROSERVOELASTIC STABILITY ANALYSIS
 ALT = S.L., M = 0.9 AERODYNAMICS - GBU-8 STORE

VELOCITY M/S (KTS)	YAW LOOP STABILITY	ROLL LOOP	
		GAIN AND PHASE MARGINS	PHASE MARGIN
		GAIN CROSSOVER	
204 (396)	STABLE	0.14	+100°
238 (462)	STABLE	0.20	+97°
271 (528)	STABLE	0.30	+35°
305 (594)	UNSTABLE	-	-
305*(594*)	STABLE	0.463	+24°

* WITH 0.02 DAMPING IN FLEXIBLE MODES

TABLE 6.- B-61 CONFIGURATION SYMMETRIC MODE FREQUENCIES

DESCRIPTION	PRODUCTION PYLON (HZ)	DECOUPLER PYLON K=3502 N/CM (2000 LB/IN) (HZ)	DECOUPLER PYLON ZERO PITCH STIFFNESS (HZ)
WING BENDING	6.08	5.99	6.02
B-61 PITCH	9.33	6.19	
FUSELAGE BENDING	11.68	11.57	11.39
LAUNCHER PITCH	12.65	12.46	12.12
B-61 YAW	13.07	11.29	11.26
2nd WING BENDING		13.94	13.22
WING OUTER PANEL TORSION	18.318	19.968	19.87
2nd LAUNCHER PITCH	20.24		
HORIZONTAL TAIL BENDING	20.47	20.48	20.47

TABLE 7. - B-61 CONFIGURATION ANTISYMMETRIC MODE FREQUENCIES

DESCRIPTION	PRODUCTION PYLON HZ	DECOUPLER PYLON HZ K=3502 N/CM (2000 LB/IN)	DECOUPLER PYLON ZERO PITCH STIFFNESS HZ
B-61 PITCH	9.043	6.11	
WIND BENDING	10.09	9.82	9.74
VERT. TAIL BENDING	12.30	12.36	12.38
B-61 YAW	12.69	11.31	11.31
FUSELAGE LATERAL BENDING	14.51	15.48	15.05
LAUNCHER PITCH	14.25	14.41	14.41
HORIZONTAL TAIL BENDING	19.05	19.79	19.73
VERTICAL TAIL - LAT. FUSELAGE		12.44	
WING TORSION			11.63

TABLE 8.- B-61 CONFIGURATION FLUTTER ANALYSIS RESULTS
(ALTITUDE - SEA LEVEL, $g = .02$).

	M = 0.6		M = 0.9		M = 1.2	
	VELOCITY M/S (KTS)	FREQ HZ	VELOCITY M/S (KTS)	FREQ HZ	VELOCITY M/S (KTS)	FREQ HZ
PRODUCTION PYLON						
SYMMETRIC	764 (1485)	8.2	>926 (>1800)		726 (1411)	7.9
ANTISYMMETRIC	329 (640)	9.6	334 (649)	9.5	293 (570)	9.7
DECOUPLER PYLON						
SYMMETRIC	241 (469)	6.1	253 (492)	6.1	215 (417)	6.1
ANTISYMMETRIC	691 (1343)	6.4	681 (1324)	6.4	>720 (>1400)	

TABLE 9.- FLIGHT CONTROL SYSTEM ROLL CHANNEL STABILITY MARGINS - B-61 CONFIGURATION

VELOCITY M/S (KTS)	GAIN CROSSOVER	PHASE MARGIN	FREQUENCY HZ
204 (397)	0.186	HIGH	3.02
	0.148	HIGH	4.67
305 (594)	0.210	HIGH	2.80
	0.630	HIGH	4.66

TABLE 10.- MODE FREQUENCIES OF THE MODEL B-61 STORE CONFIGURATION.

DESCRIPTION	FSS WINGS HZ	ORIGINAL WINGS HZ
<u>SYMMETRIC MODES</u>		
WING BENDING	10.88	10.91
B-61 PITCH	15.52	15.60
B-61 YAW	17.44	17.57
LAUNCHER PITCH	19.15	19.15
FUSELAGE BENDING	25.81	25.87
<u>ANTISYMMETRIC MODES</u>		
WING BENDING	14.62	14.67
B-61 PITCH	15.82	15.87
B-61 YAW	17.61L 17.29R 17.56*	17.09L 17.21R 17.05*
LAUNCHER PITCH	20.97	20.99
LEFT HORIZONTAL TAIL	27.69	
BOTH HORIZONTAL TAILS		28.30

* Complete mode for this frequency is shown in Appendix C.

TABLE 11.- NASA DECOUPLER PYLON WIND TUNNEL TEST SUMMARY.

DATE	RUN NO.	TUNNEL RUN NO.	MODEL STORE CONFIGURATION			TUNNEL HEAD PRESS (PSF)	MAX. MACH NO.	DYN. PRESS. Q	RESULTS
			WING STA. 1 & 9	WING STA. 3 & 7	WING STA. 4 & 6				
8-1-83	1	34	AIM-9 (AIM-9 Launcher)	GBU-8 (Production Pylon)	370 Gal Tank (1/2 Full) (Tank Pylon)	300	0.678	(PSF) 62.0	Antisym. Flutter @ 8.6 Hz
						400	0.61	69.4	Antisym. Flutter @ 8.6 Hz
						500	0.56	74.2	Antisym. Flutter @ 8.6 Hz
						500	0.57	76.7	Cable tension was reduced from 500 lbs to 400 lbs
						700	0.53	92.0	Antisym. Flutter @ 8.6 Hz
						800	0.54	110.5	Antisym. Flutter @ 8.6 Hz
8-2-83	2	35	AIM-9 (AIM-9 Launcher)	GBU-8 (Production Pylon)	370 Gal Tank (Full) (Tank Pylon)	300	0.76	80.5	Antisym. Flutter @ 8.3 Hz
						400	0.70	87.1	Antisym. Flutter @ 8.3 Hz (above mild level)
						500	0.65	93.3	Antisym. Flutter @ 8.3 Hz
						650	0.60	103.0	Antisym. Flutter @ 8.3 Hz
						800	0.58	125.9	Antisym. Flutter @ 8.3 Hz
8-3-83	3	36	AIM-9's (AIM-9 Launcher)	GBU-8 (Decoupler Pylon)	370 Gal Tank (Full)	350	0.90	101.9	No Flutter
						400	0.95	135.2	No Flutter (Significant Sym. Motion @ 5.6 Hz was observed)
						500	0.90	159.0	No Flutter
8-3-83	4	37	AIM-9 Launcher (Only)	B-61 (Production Pylon)		400	1.10	151.0	No Flutter (Buffet was encountered @ M=0.85 to 0.95)
						500	1.00	180.0	No Flutter (Buffet was encountered @ M = 0.85 to 0.95)
8-4-83	5	38	AIM-9's (AIM-9 Launcher)	GBU-8 (Decoupler Pylon with equivalent 6000" # breakout (Friction) Pitch Mom.)	370 Gal Tank (Full)	300	0.95	109.0	No Flutter
				Approx same as measured on full scale article.		400	0.95	135.0	No Flutter
						500	0.90	162.0	No Flutter (Less sym motion than noted in Run 36)

TABLE 11.- (CONTINUED).

DATE	RUN NO.	TUNNEL RUN NO.	MODEL STORE CONFIGURATION			TUNNEL HEAD PRESS (PSF)	MAX. MACH NO	DYN. PRESS. Q (PSF)	RESULTS
			WING STA. 1 & 9	WING STA. 3 & 7	WING STA. 4 & 6				
8-4-83	6	39	AIM-9's (AIM-9 Launcher)	GBU-8 (Decoupler Pylon with same friction as in Run No. 38)	370 Gal Tank (1/2 Full)	300 400 500	0.95 0.957 0.90	108.7 136.1 161.8	No Flutter No Flutter (Buffet occurred @ M = 0.85) No Flutter
8-5-83	7	41	AIM-9's (AIM-9 Launchers)	GBU-8 (Decoupler Pylons with equivalent 12,000" # breakout (Friction) pitch mom.)* * Approx. 1/2 of breakout friction was lost during run.	370 Gal Tank (Full)	300 400 500	0.95 0.95 0.90	108.8 135.1 161.1	No Flutter (Some motion @ 8.1 Hz at high dynamic press.) No Flutter No Flutter

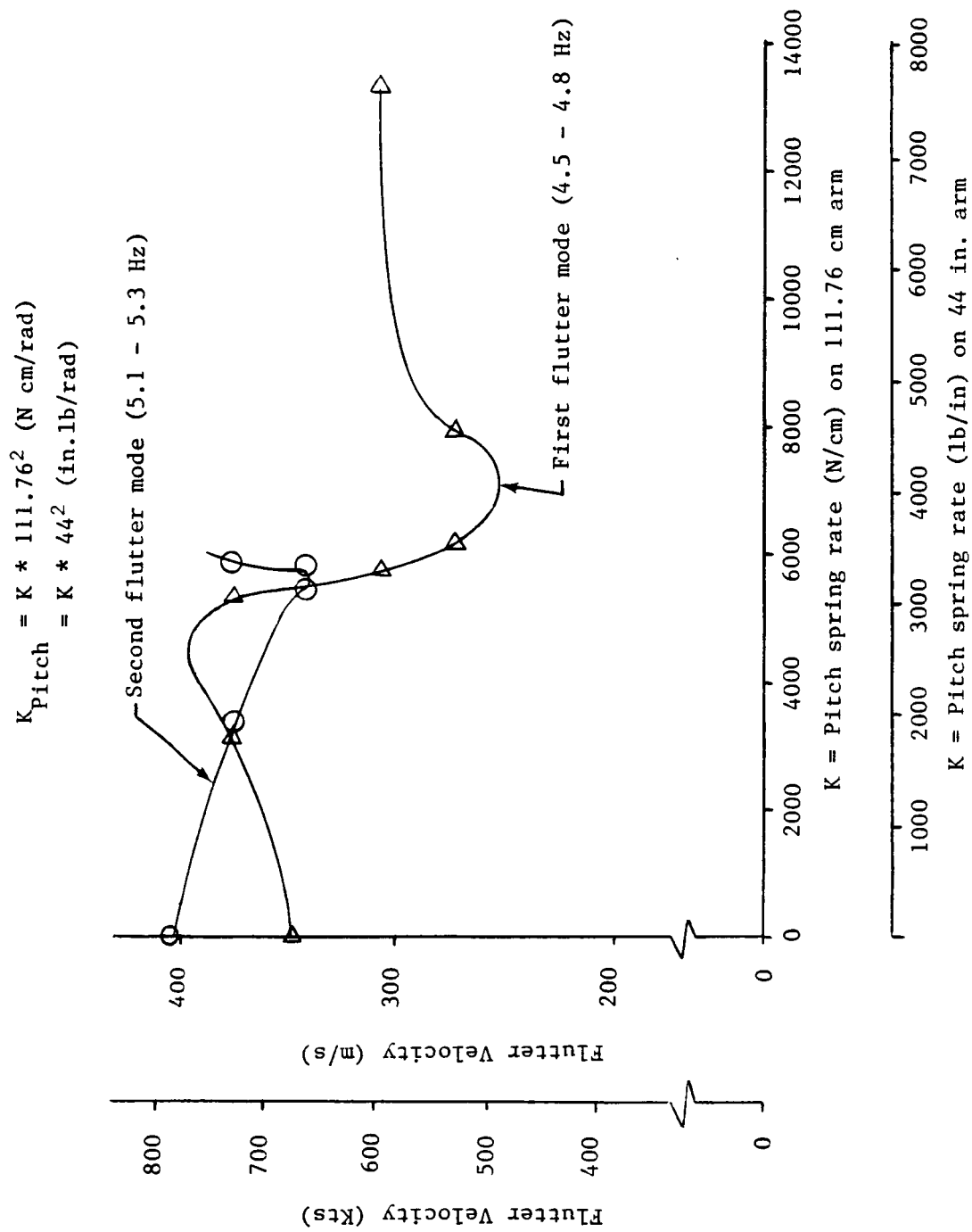


Figure 1.- Antisymmetric airframe flutter speeds.

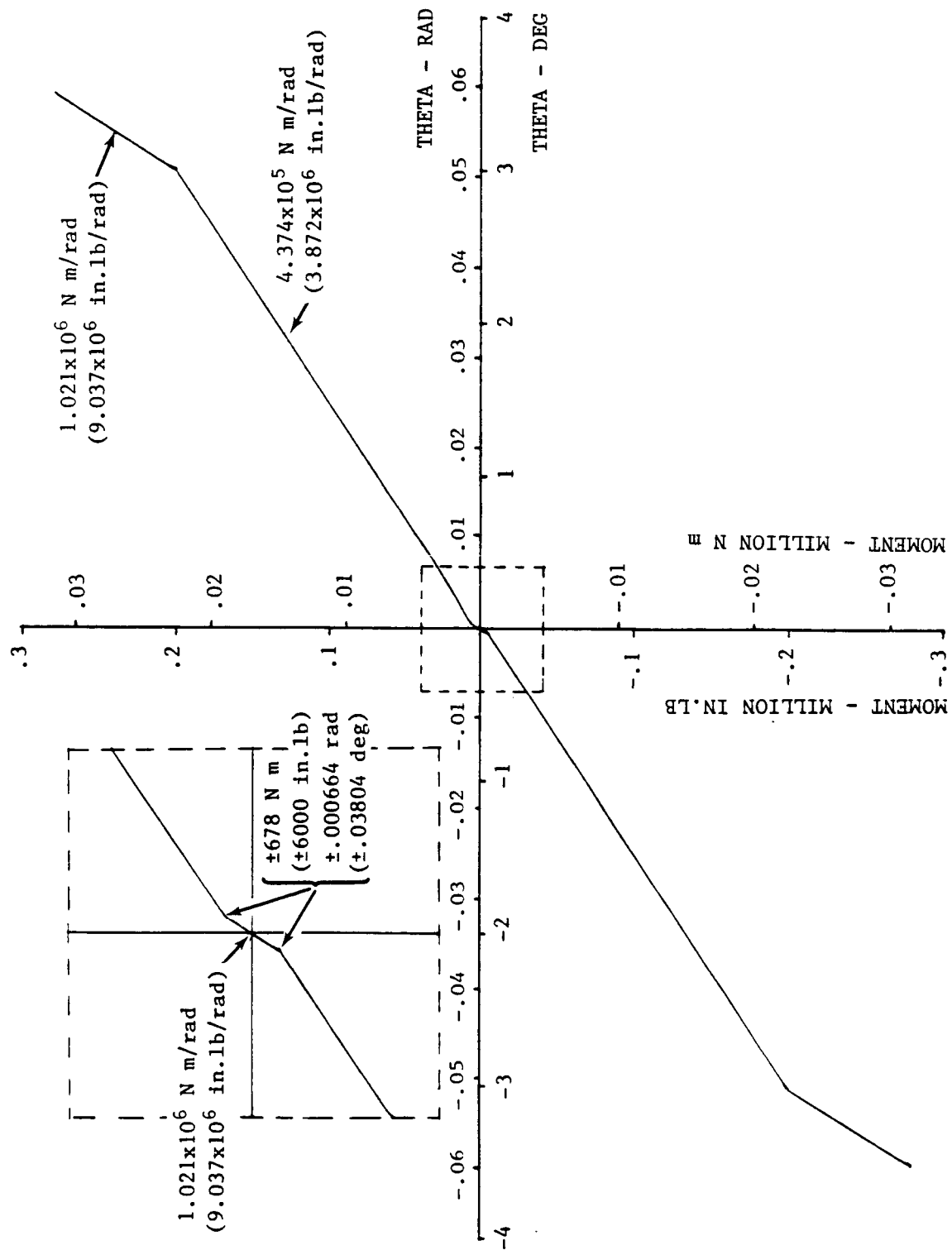


Figure 2.- Nonlinear spring rate including friction effects.

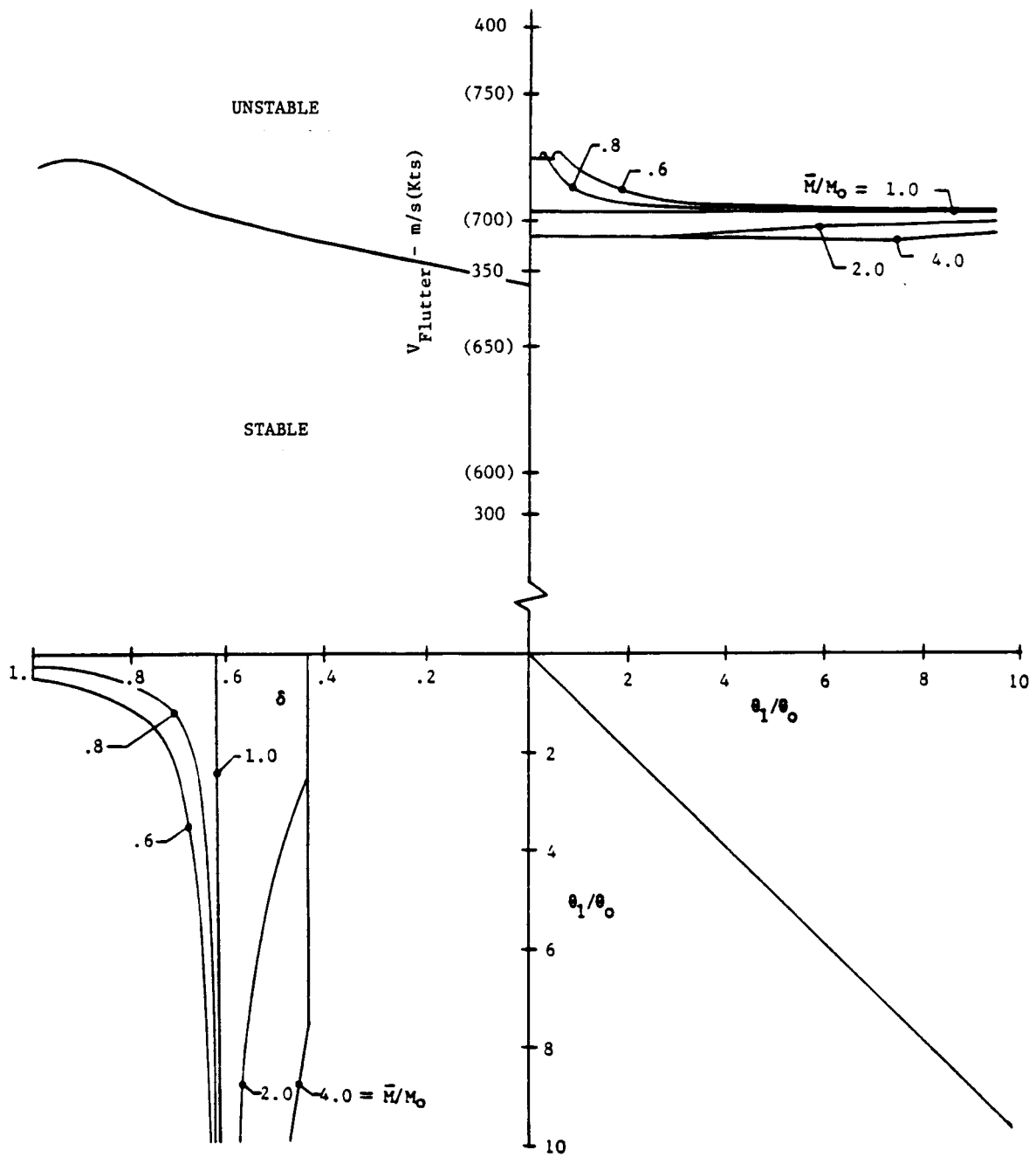


Figure 3.- Flutter boundary determination with non-linear spring rate.

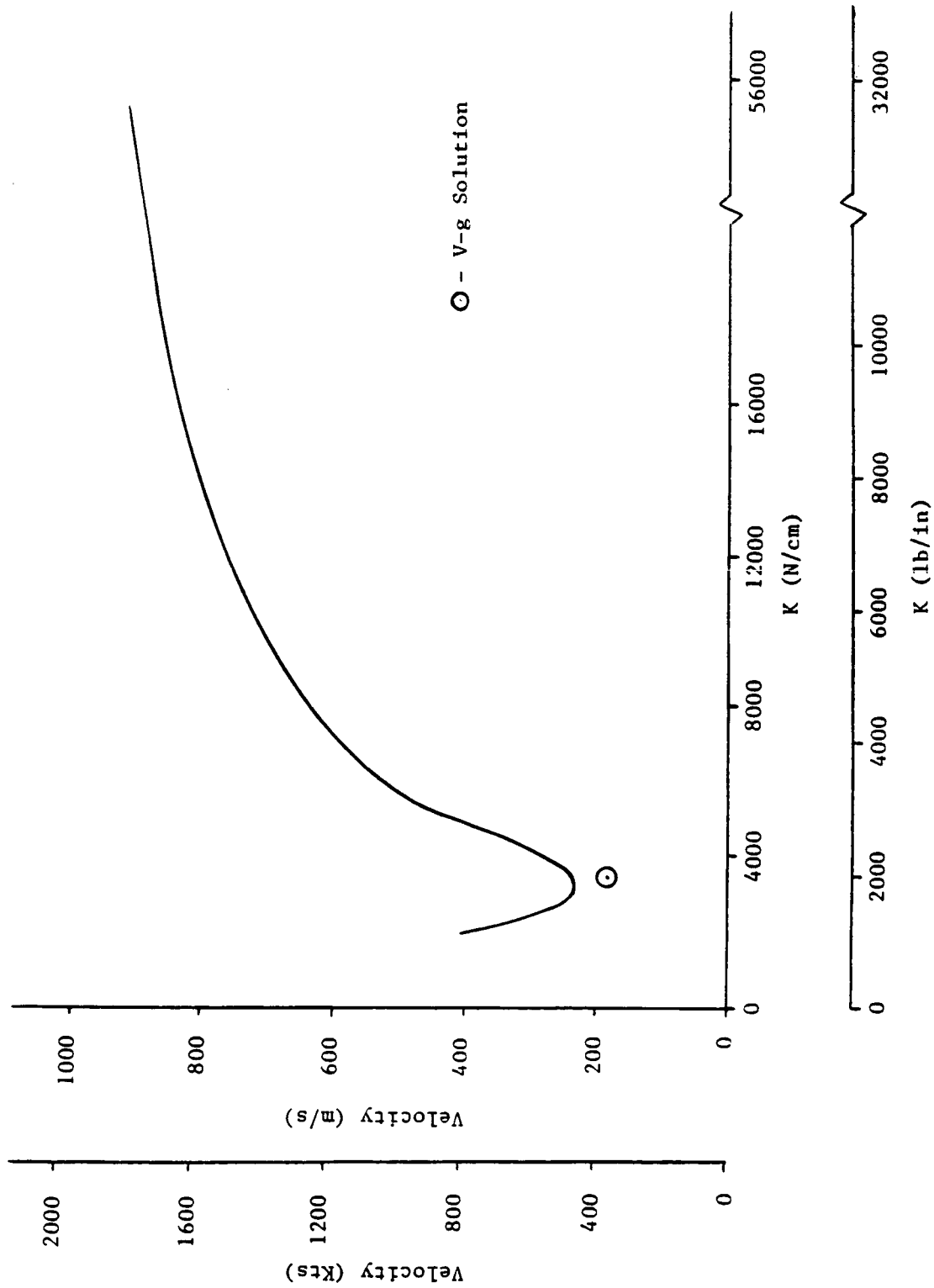


Figure 4.- Effect of pylon pitch spring rate on symmetric flutter velocity -
B-61 store, $M=0.9$.

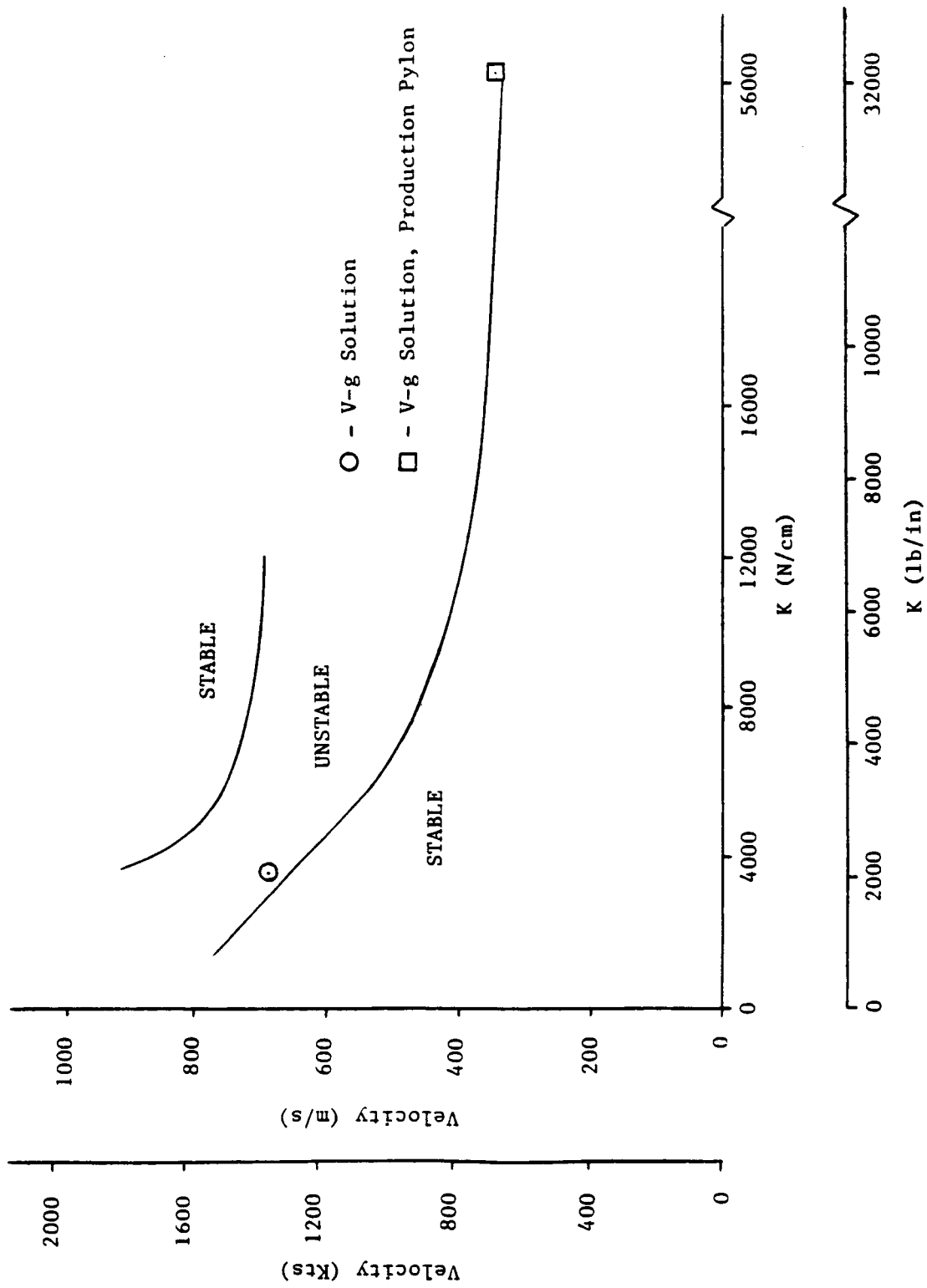


Figure 5.- Effect of pylon pitch spring rate on antisymmetric flutter velocity -
B-61 store, $M=0.9$.

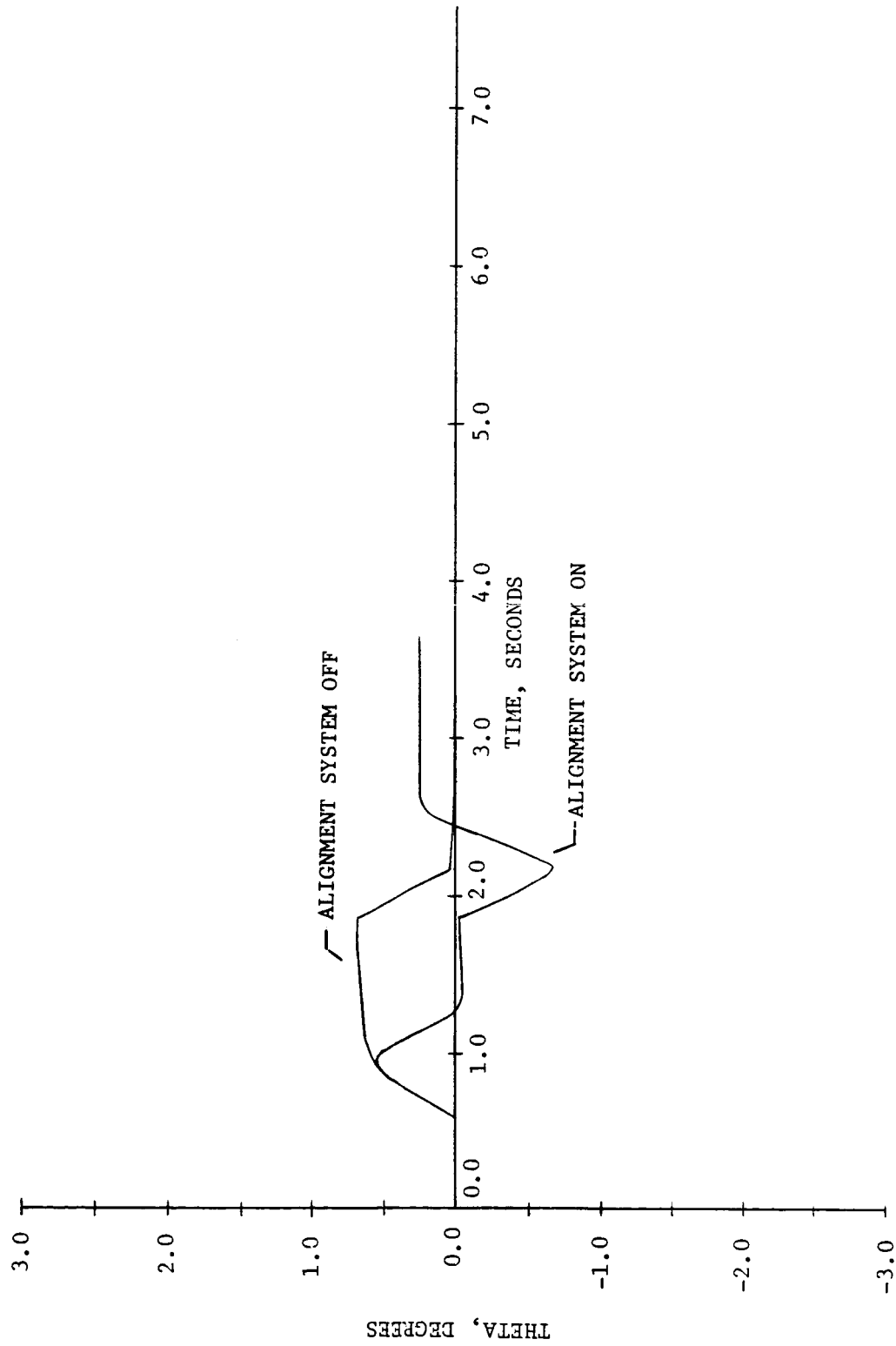


Figure 6.- Predicted alignment system performance, B-61 configuration -
4.4 g roll, $K = 3502 \text{ N/cm}(2000 \text{ lb/in})$.

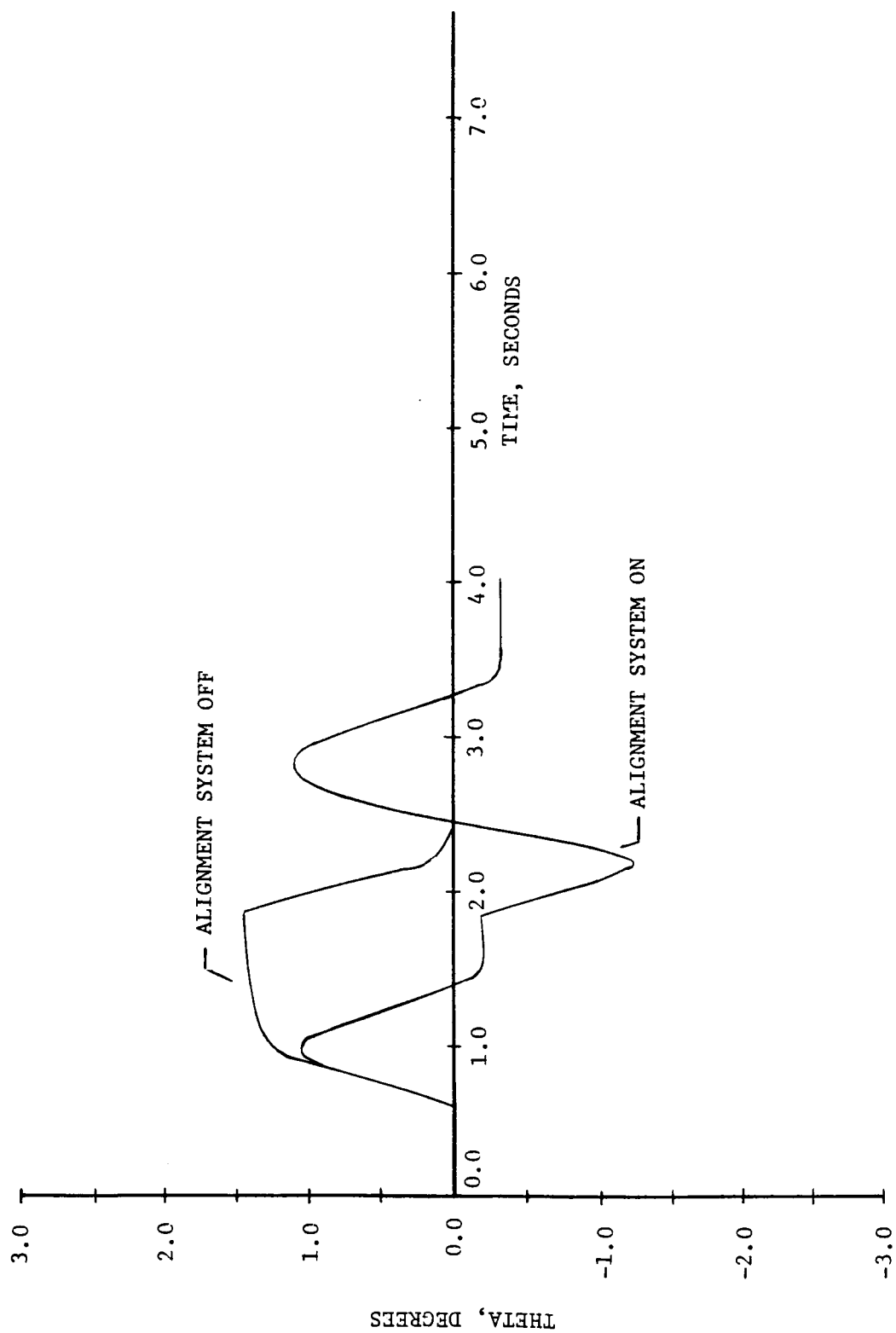


Figure 7.- Predicted alignment system performance, B-61 configuration -
4.4 g roll, $K = 1750 \text{ N/cm}(1000 \text{ lb/in})$.

ORIGINAL PAGE IS
OF POOR QUALITY

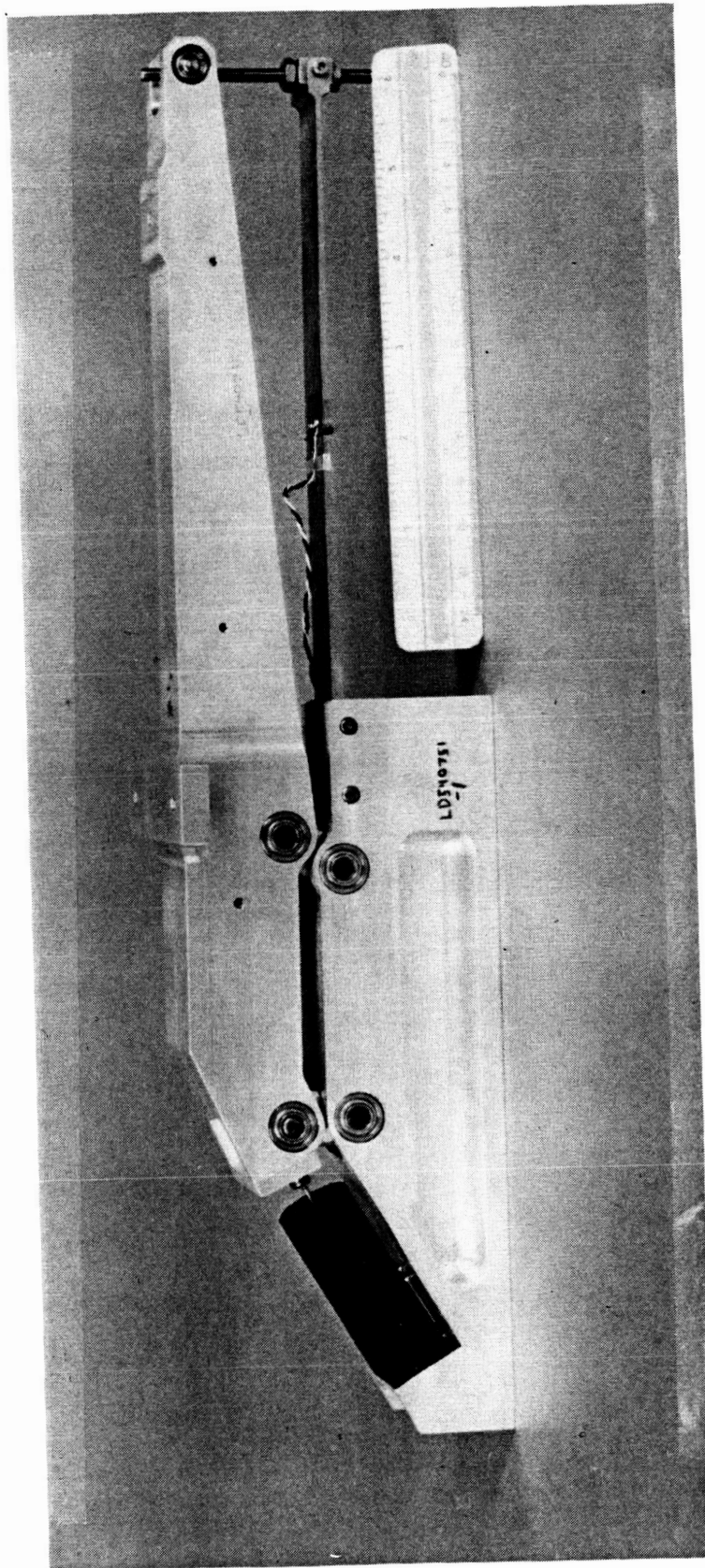


Figure 8.- 1/4 Scale model decoupler pylon internal arrangement.

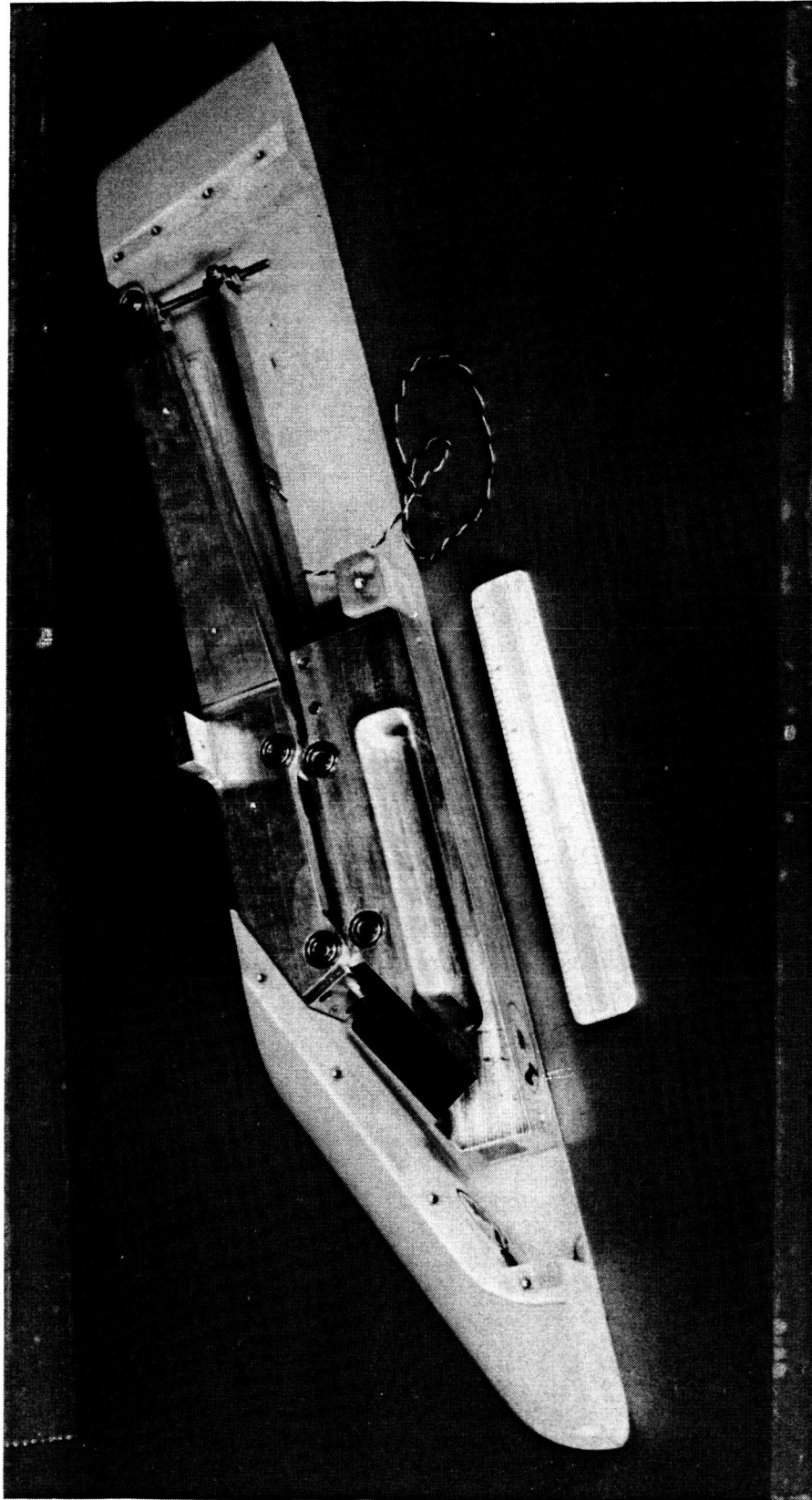


Figure 9.- 1/4 Scale model decoupler pylon with side fairing removed.

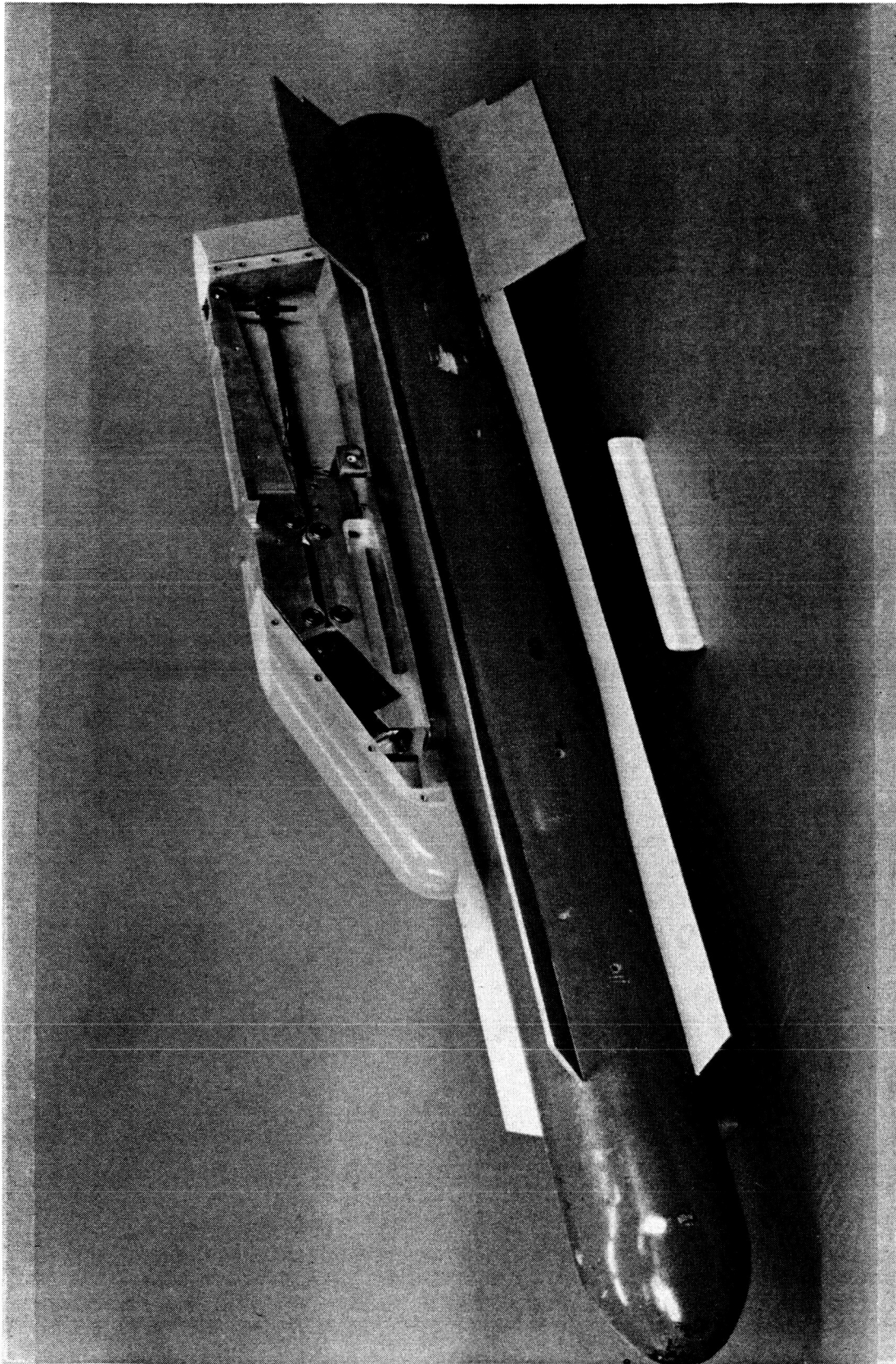


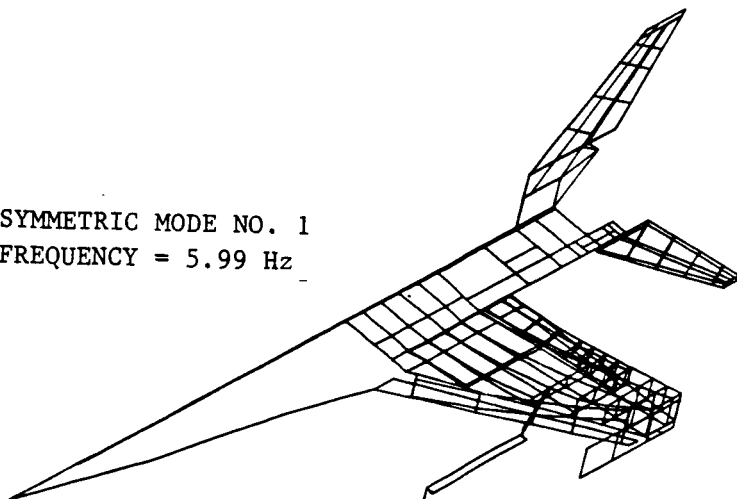
Figure 10.- 1/4 Scale model decoupler pylon and GBU-8 weapon.

APPENDIX A

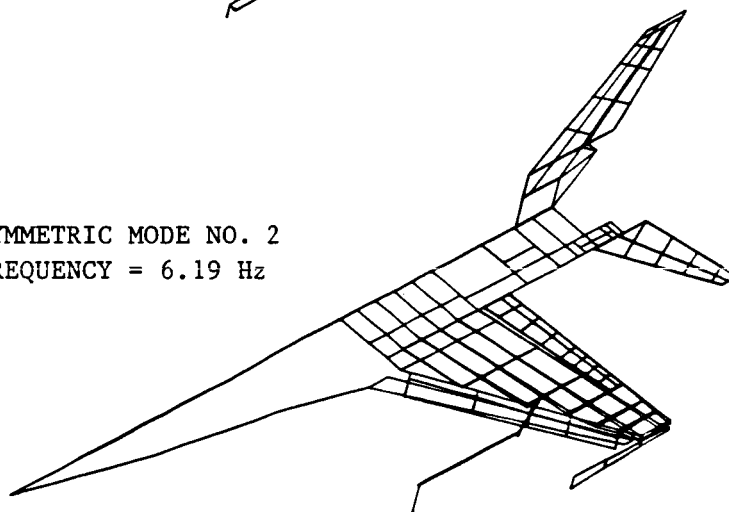
Symmetric Modes for B-61 on Decoupler Pylon

This appendix contains the computed symmetric mode shapes for the first three frequencies with the B-61 store on the decoupler pylon. Modes were computed for zero pitch stiffness as well as for 3502 N/cm (2000 lb/in.) pitch stiffness.

SYMMETRIC MODE NO. 1
FREQUENCY = 5.99 Hz



SYMMETRIC MODE NO. 2
FREQUENCY = 6.19 Hz



SYMMETRIC MODE NO. 3
FREQUENCY = 11.29 Hz

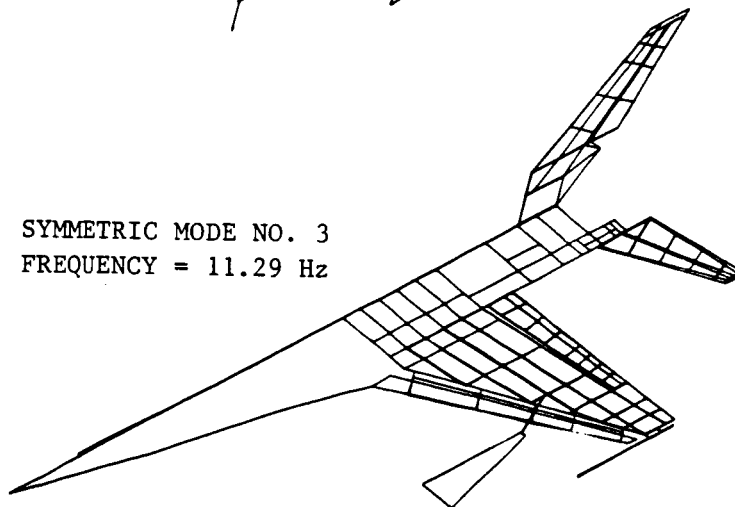
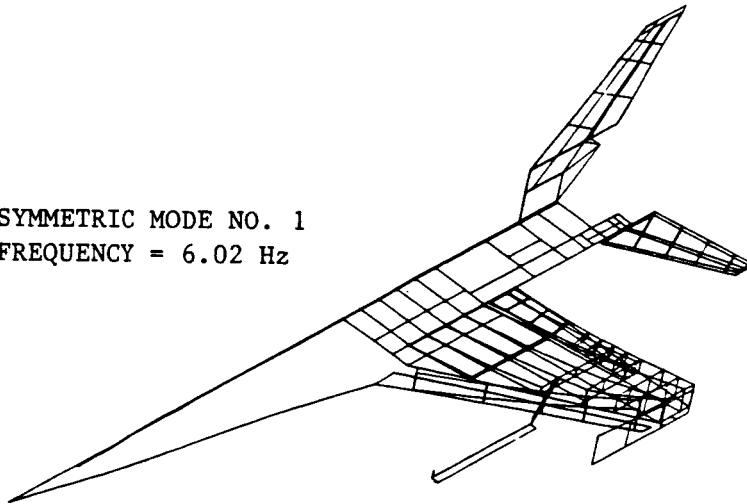
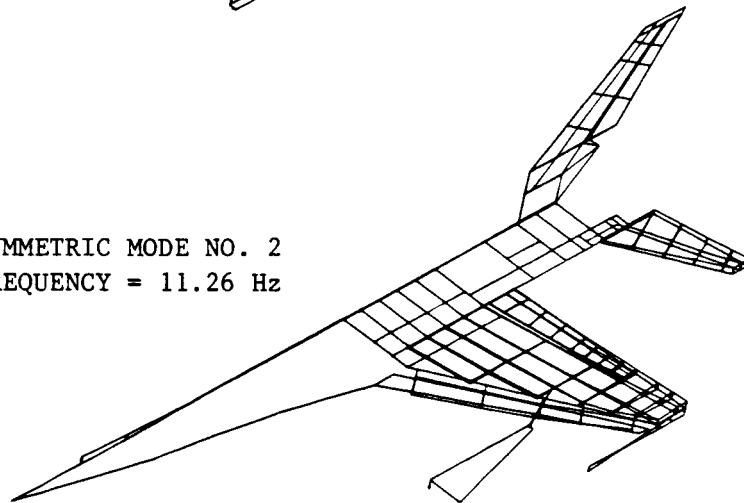


Figure A1.- First three computed symmetric modes for B-61 on decoupler pylon -
K = 3502 N/cm(2000 lb/in).

SYMMETRIC MODE NO. 1
FREQUENCY = 6.02 Hz



SYMMETRIC MODE NO. 2
FREQUENCY = 11.26 Hz



SYMMETRIC MODE NO. 3
FREQUENCY = 11.39 Hz

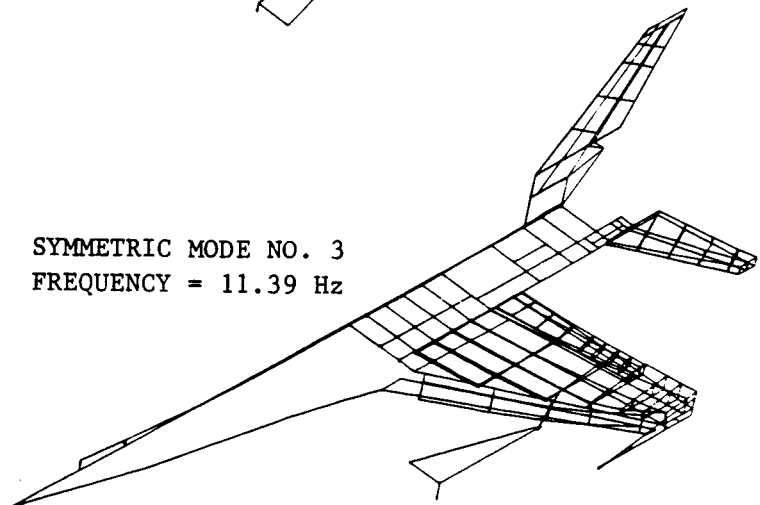


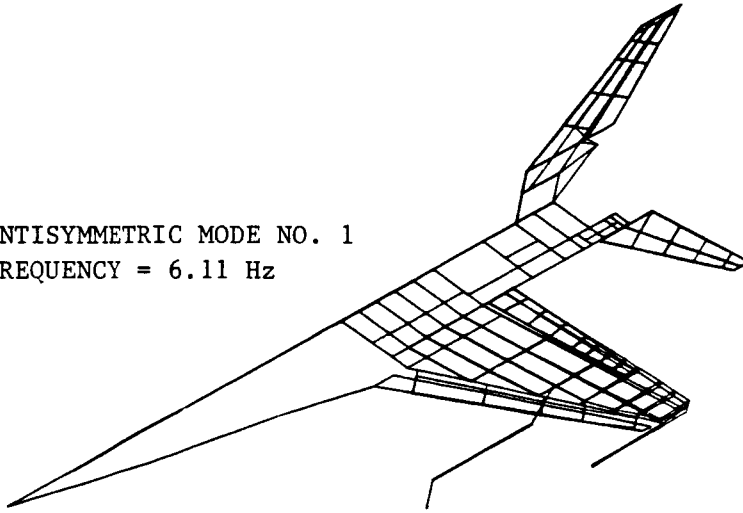
Figure A2.- First three computed symmetric modes for B-61 on decoupler pylon - with zero pitch stiffness.

APPENDIX B

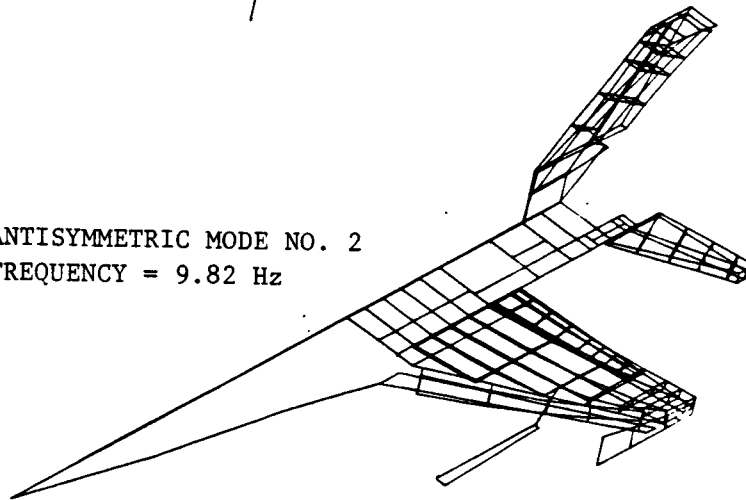
Antisymmetric Modes for B-61 on Decoupler Pylon

This appendix contains the computed antisymmetric mode shapes for the first three frequencies with the B-61 store on the decoupler pylon. Modes were computed for zero pitch stiffness as well as for 3502 N/cm (2000 lb/in.) pitch stiffness.

ANTISYMMETRIC MODE NO. 1
FREQUENCY = 6.11 Hz



ANTISYMMETRIC MODE NO. 2
FREQUENCY = 9.82 Hz



ANTISYMMETRIC MODE NO. 3
FREQUENCY = 11.31 Hz

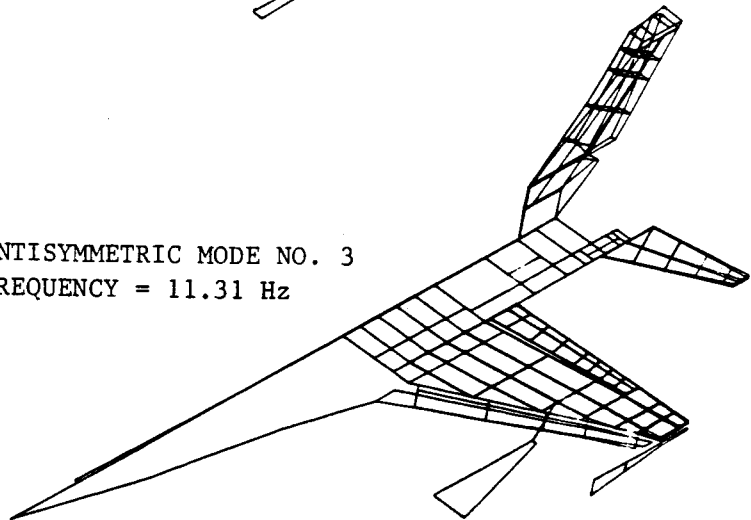
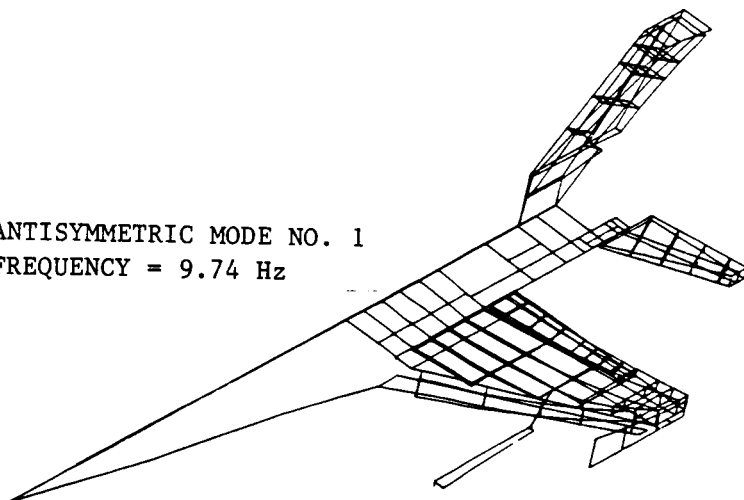
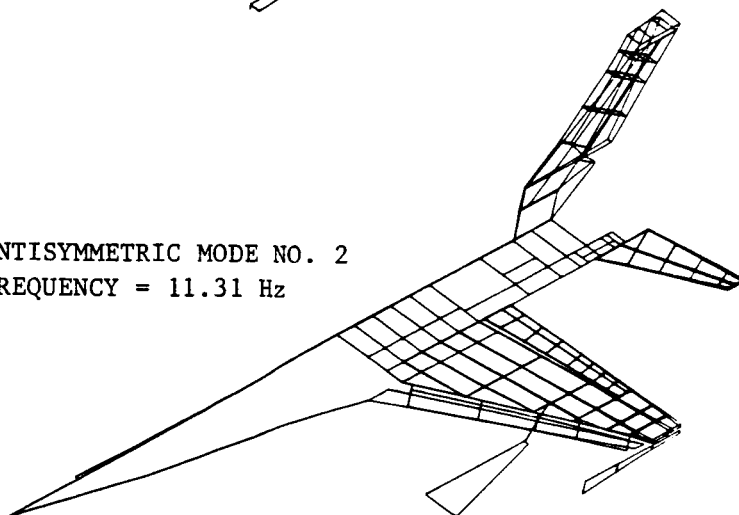


Figure B1.- First three computed antisymmetric modes for B-61 on decoupler pylon -
 $K = 3502 \text{ N/cm}(2000 \text{ lb/in})$.

ANTISYMMETRIC MODE NO. 1
FREQUENCY = 9.74 Hz



ANTISYMMETRIC MODE NO. 2
FREQUENCY = 11.31 Hz



ANTISYMMETRIC MODE NO. 3
FREQUENCY = 11.63 Hz

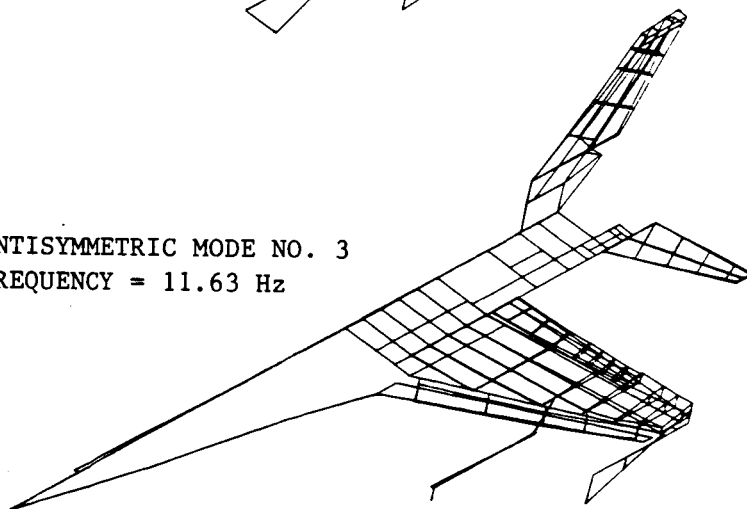


Figure B2.- First three computed antisymmetric modes for B-61 on decoupler pylon - with zero pitch stiffness.

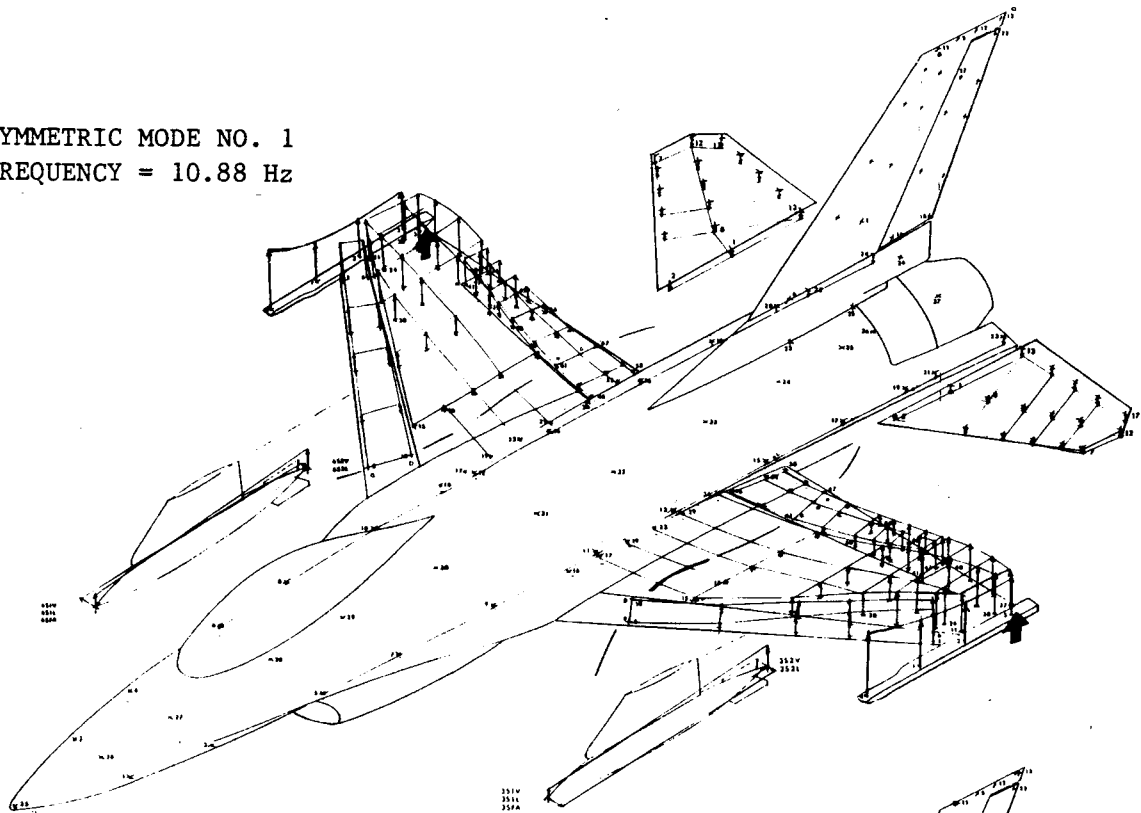
APPENDIX C

Model Ground Vibration Test Modes

This appendix contains measured model ground vibration test (GVT) modes for the B-61 store and decoupler pylon on the flutter suppression wings and on the original wings. Symmetric and antisymmetric modes are shown.

ORIGINAL PAGE IS
OF POOR QUALITY

SYMMETRIC MODE NO. 1
FREQUENCY = 10.88 Hz



SYMMETRIC MODE NO. 2
FREQUENCY = 15.52 Hz

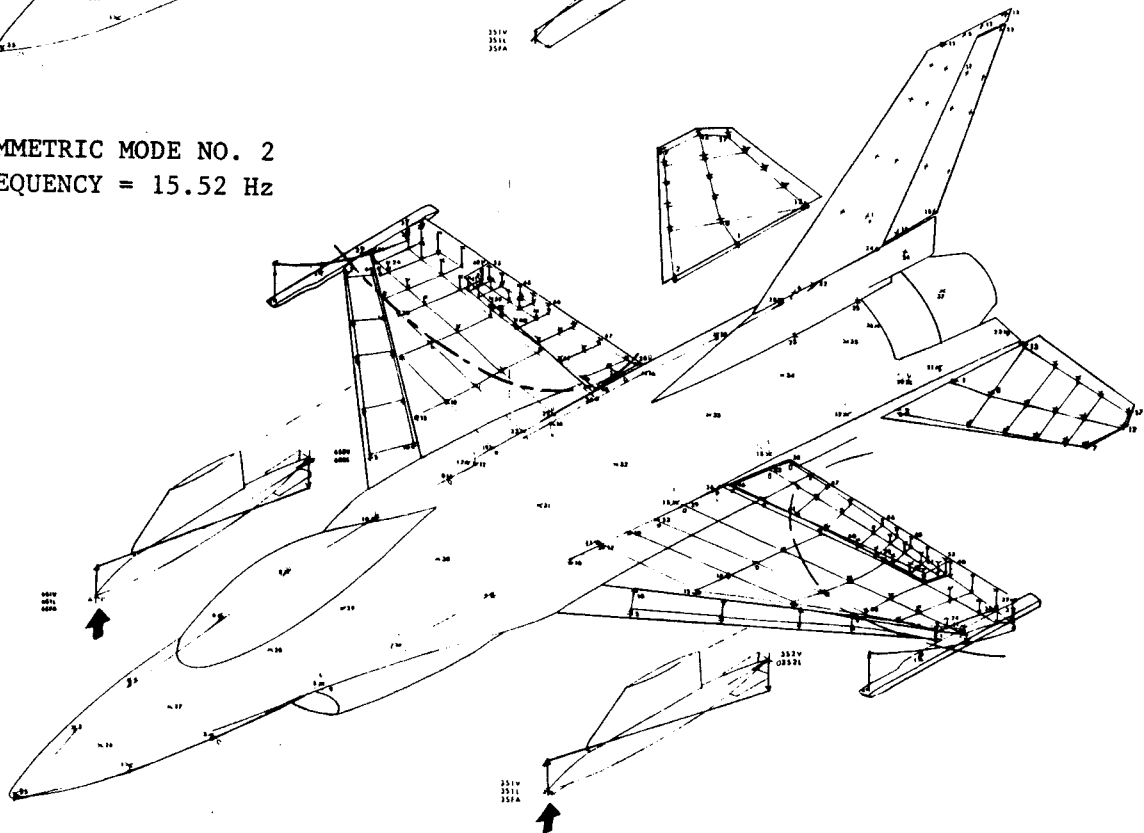
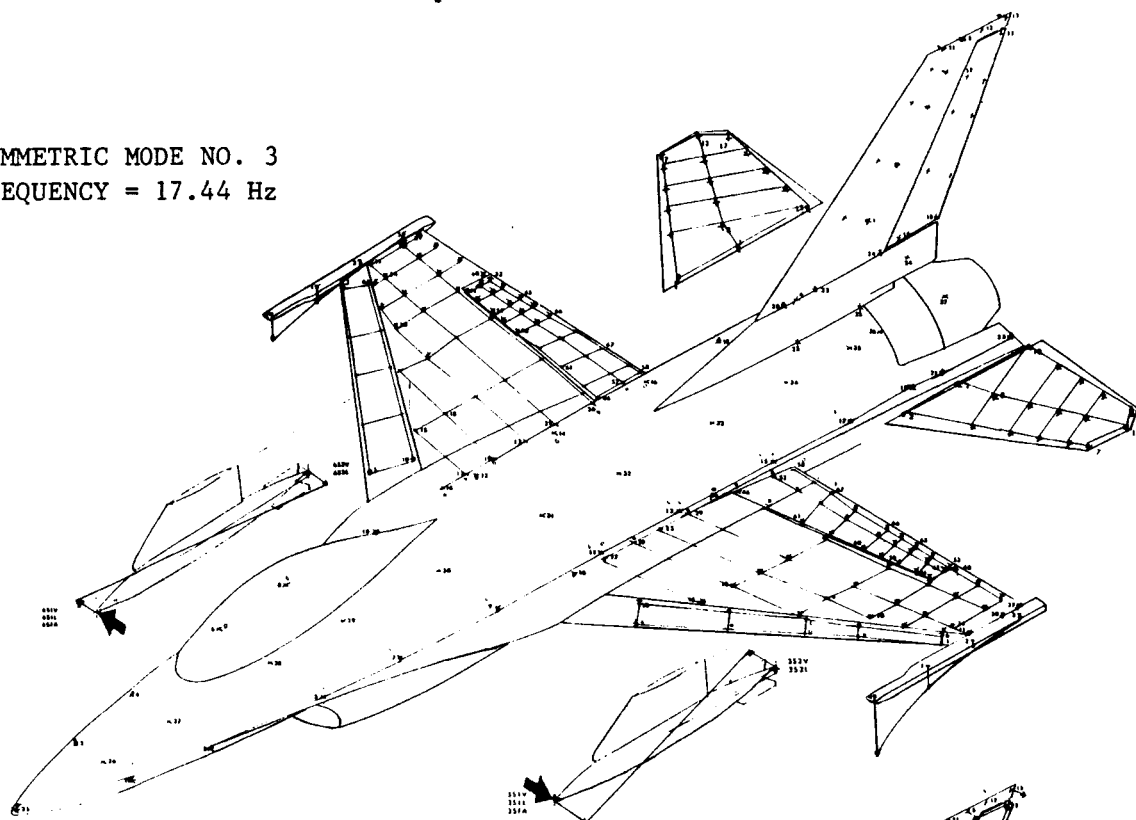


Figure C1.- GVT Symmetric Modes for Model with Flutter Suppression Wings
B-61 store.

SYMMETRIC MODE NO. 3
FREQUENCY = 17.44 Hz



SYMMETRIC MODE NO. 4
FREQUENCY = 19.15 Hz

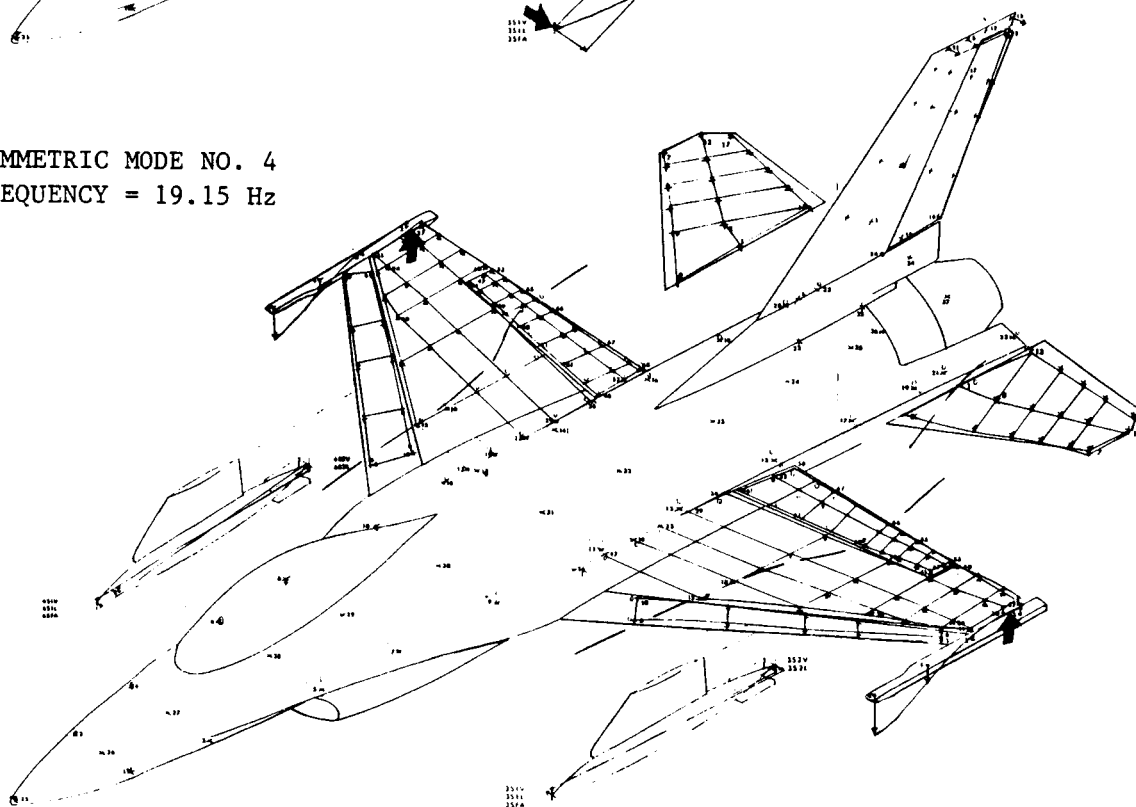


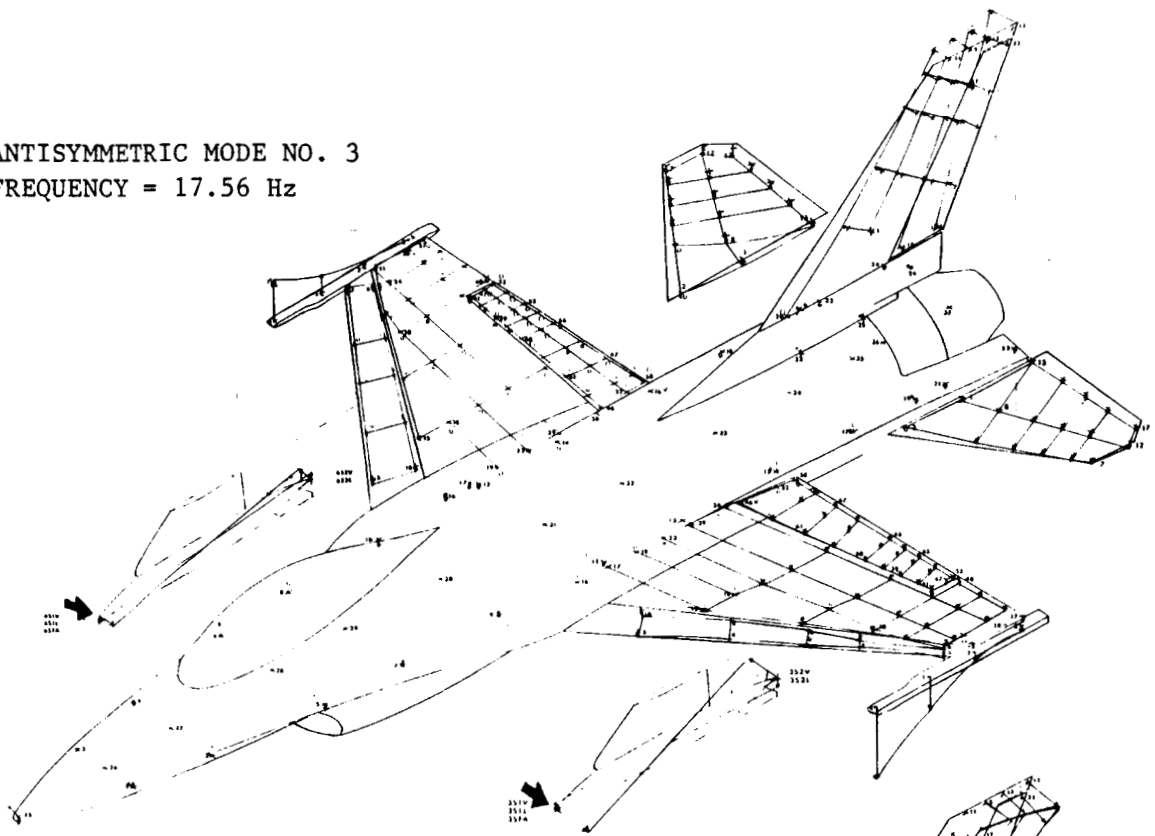
Figure C1.- (Concluded)

ANTISYMMETRIC MODE NO. 1
FREQUENCY = 14.62 Hz

351W
351A
352A

Figure C2.- GVT Antisymmetric Modes for Model with Flutter Suppression Wings.
B-61 store.

ANTISYMMETRIC MODE NO. 3
 FREQUENCY = 17.56 Hz



ANTISYMMETRIC MODE NO. 4
 FREQUENCY = 20.97 Hz

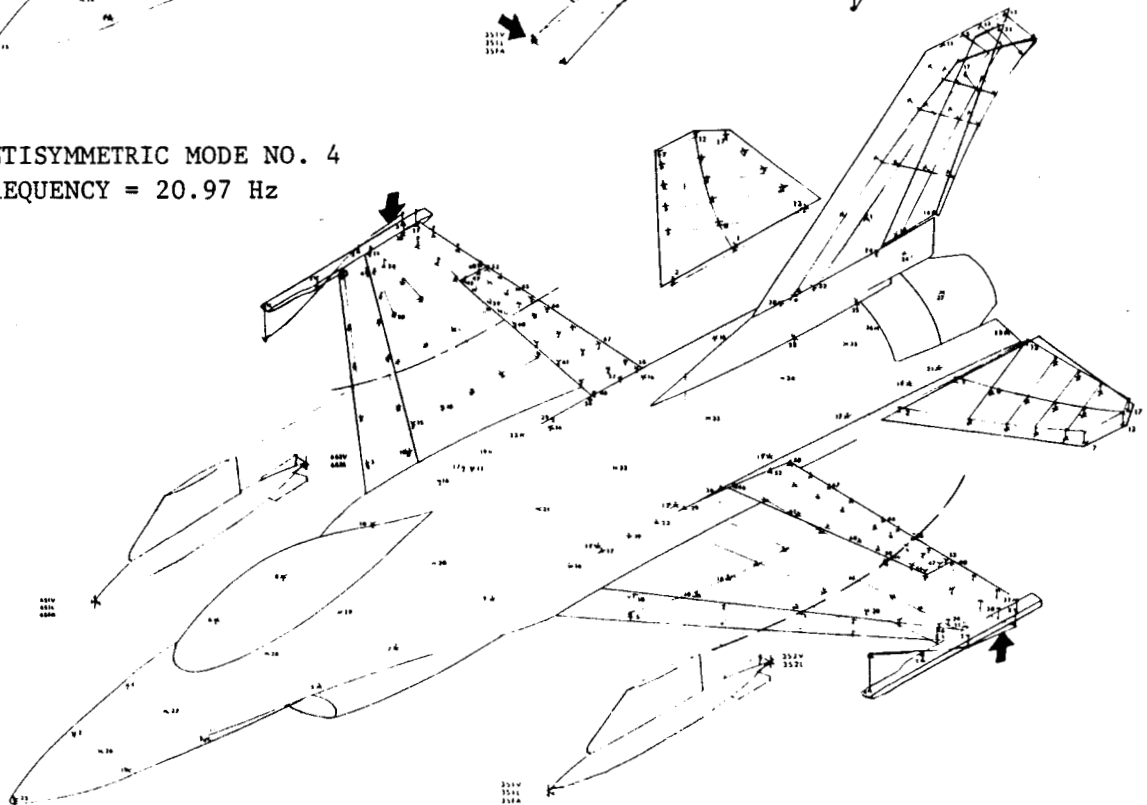
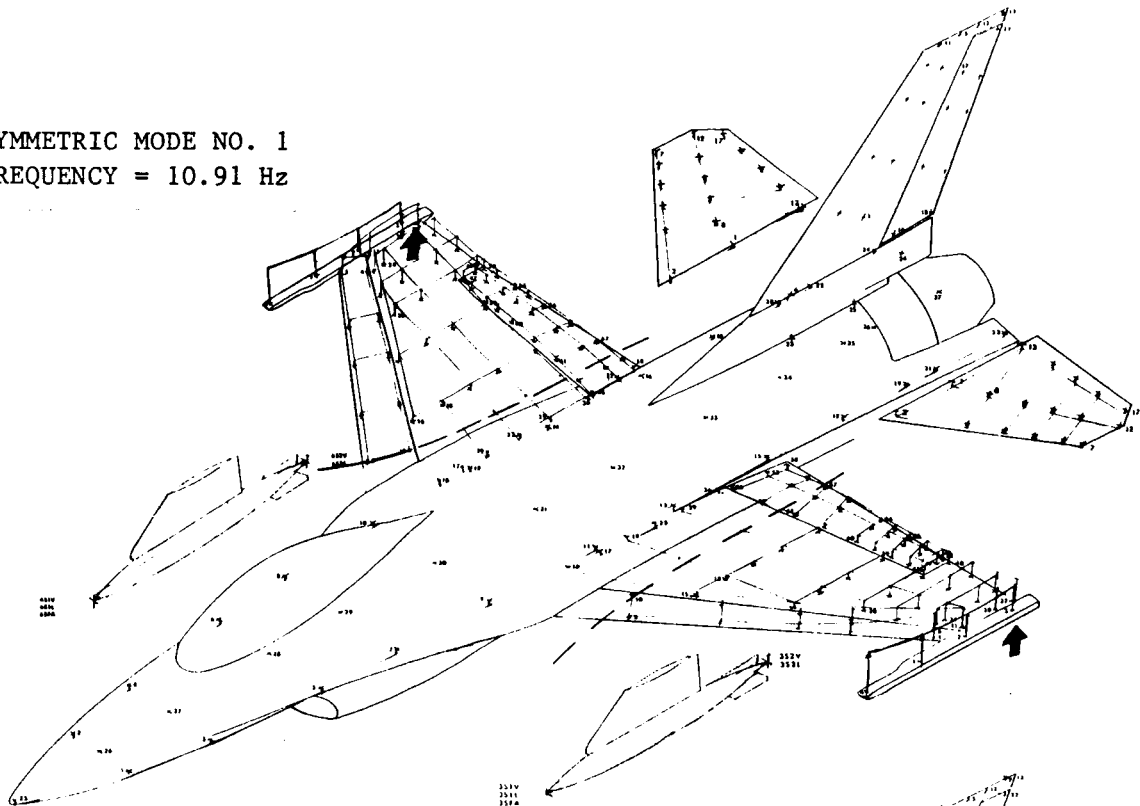


Figure C2.- (Concluded)

ORIGINAL PAGE IS
OF POOR QUALITY

SYMMETRIC MODE NO. 1
FREQUENCY = 10.91 Hz



SYMMETRIC MODE NO. 2
FREQUENCY = 15.60 Hz

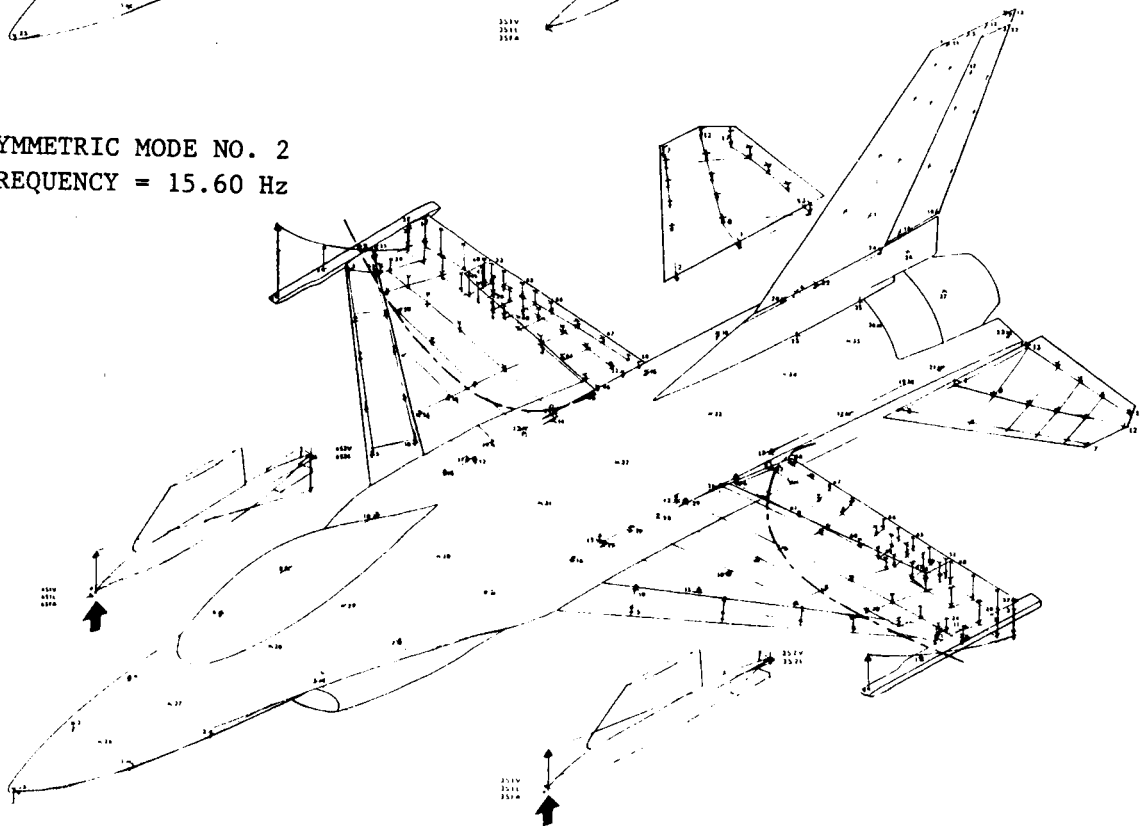
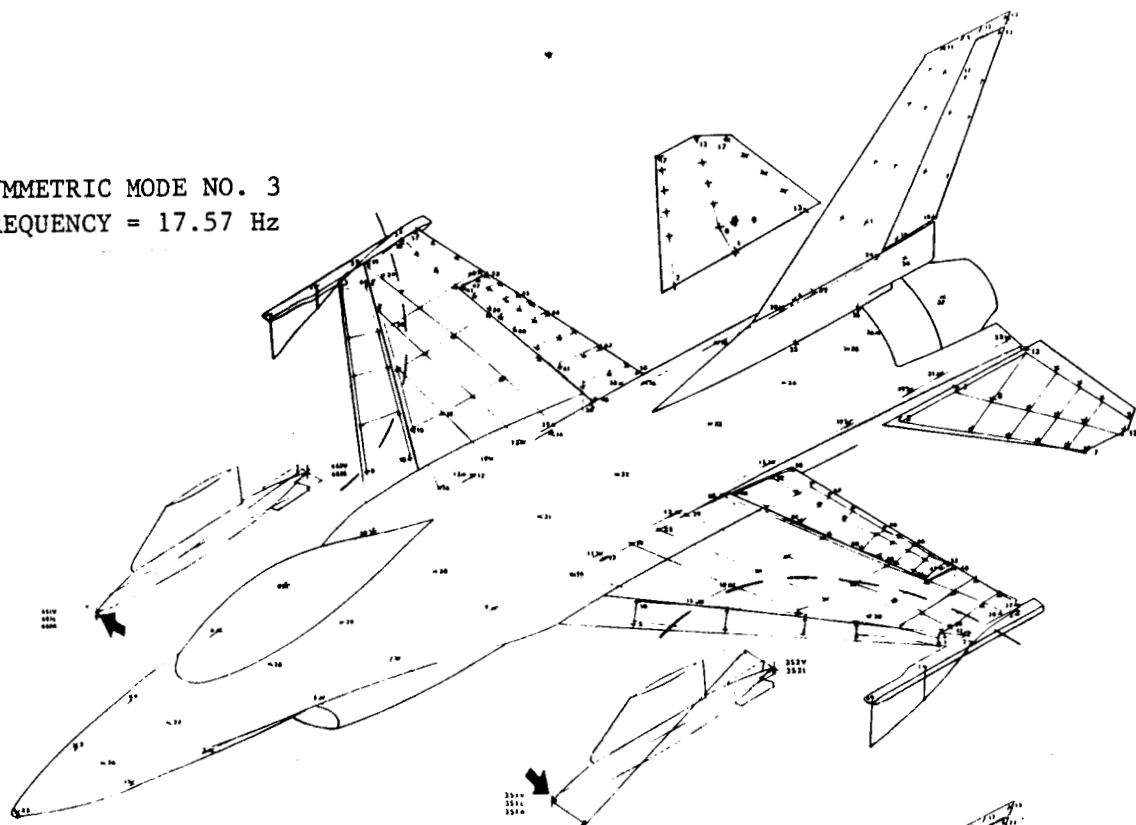


Figure C3.- GVT Symmetric Modes for Model with Original Wings
B-61 store.

SYMMETRIC MODE NO. 3
FREQUENCY = 17.57 Hz



SYMMETRIC MODE NO. 4
FREQUENCY = 19.15 Hz

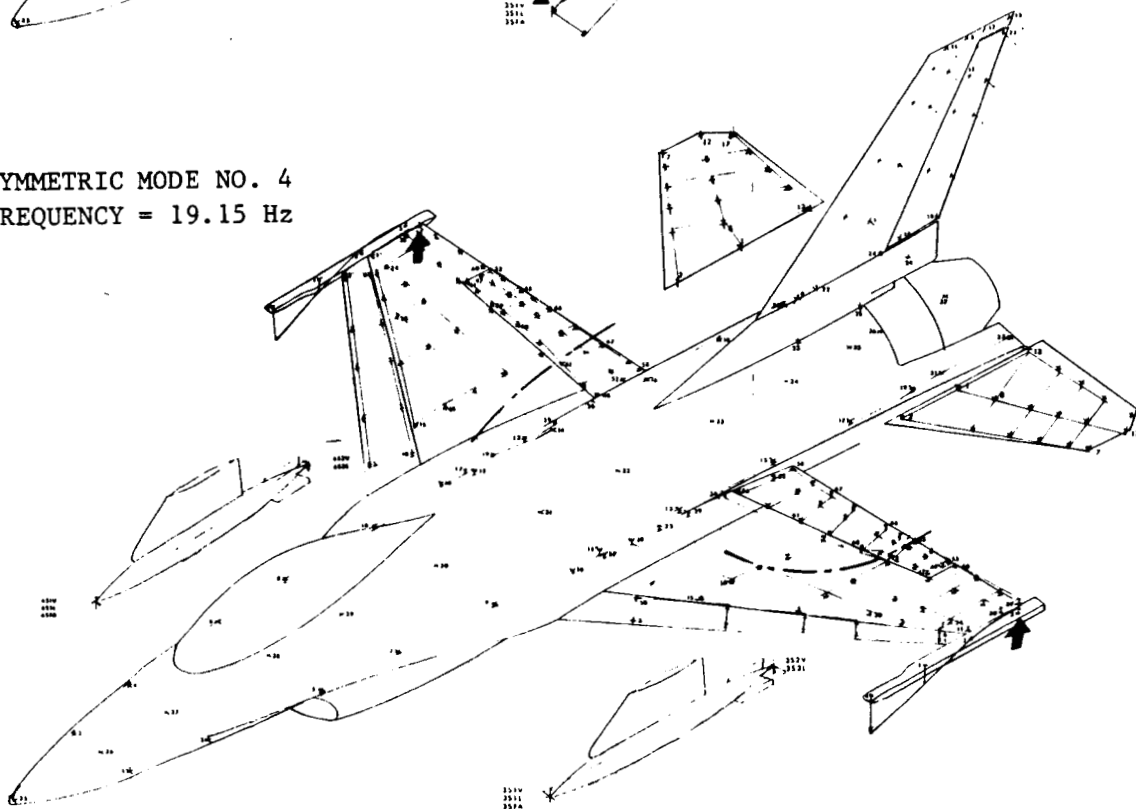
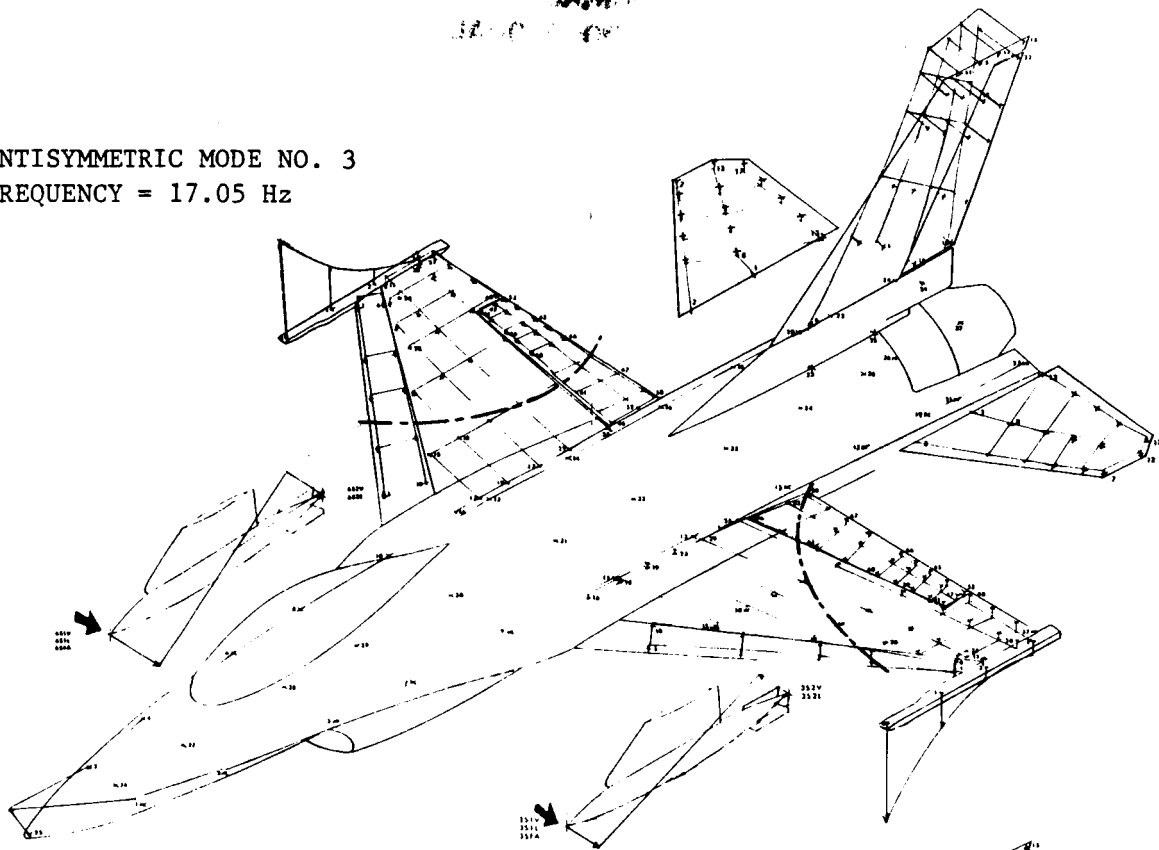


Figure C3.- (Concluded)

ANTISYMMETRIC MODE NO. 3
FREQUENCY = 17.05 Hz



ANTISYMMETRIC MODE NO. 4
FREQUENCY = 20.99 Hz

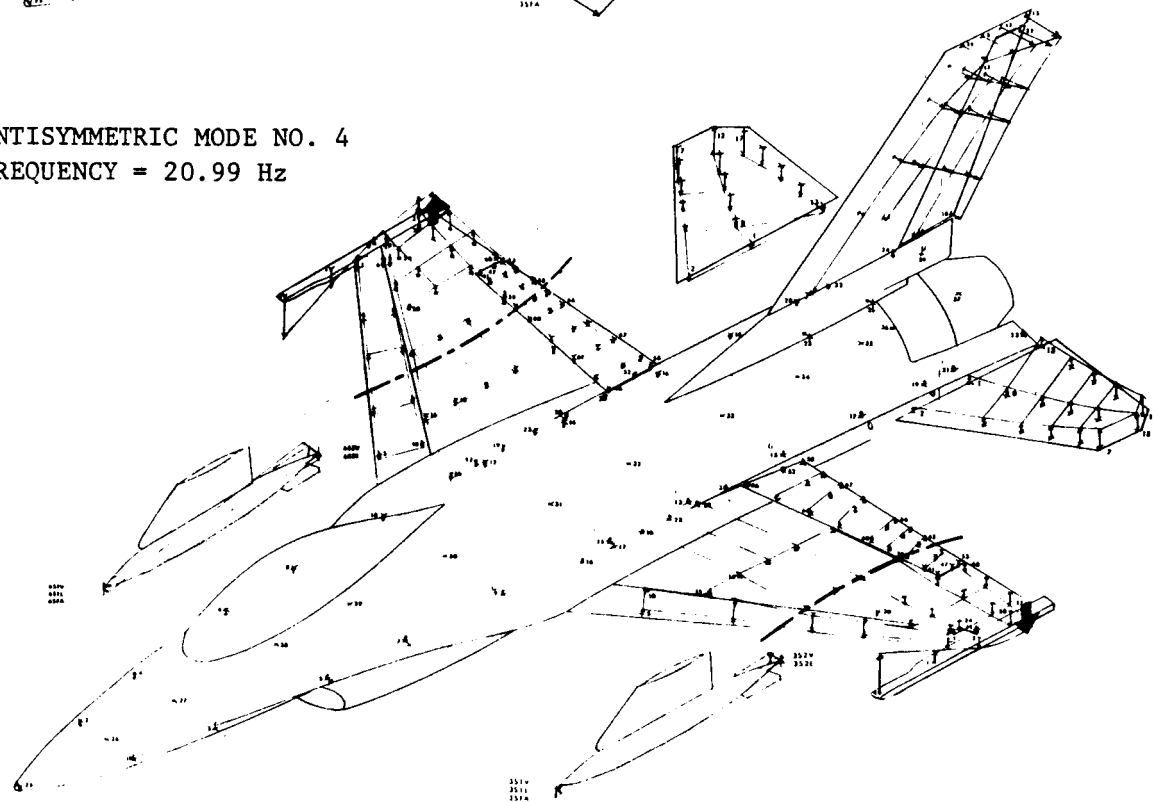




Figure C4.- (Concluded)

1. Report No. NASA CR - 172355		2. Government Accession No.		3. Recipient's Catalog No.	
4. Title and Subtitle DESIGN AND FABRICATION OF THE NASA DECOUPLER PYLON FOR THE F-16 AIRCRAFT, ADDENDUM I				5. Report Date January 1985	
				6. Performing Organization Code	
7. Author(s) J. D. Clayton and R. L. Haller				8. Performing Organization Report No.	
9. Performing Organization Name and Address General Dynamics - Fort Worth Division P. O. Box 748 Fort Worth, Texas 76101				10. Work Unit No.	
				11. Contract or Grant No. NAS1-16879	
12. Sponsoring Agency Name and Address National Aeronautics and Space Administration Washington, D.C. 20546				13. Type of Report and Period Covered Contractor Report Aug 1983 - Oct 1983	
				14. Sponsoring Agency Code 505-33-43-07	
15. Supplementary Notes Langley Technical Monitor: F. W. Cazier, Jr. Final Report					
16. Abstract The results of the final analyses which were conducted using a revised structural simulation of the Decoupler Pylon are reported in this addendum. The simulation incorporates the previously published results of ground tests performed on the flight Decoupler Pylons mounted in a test fixture at General Dynamics' Fort Worth facility. The analyses show that the Decoupler Pylon will suppress wing-store flutter for the GBU-8 flight test stores configuration on an F-16 airplane. The feasibility of carrying a B-61 on the pylons is also investigated with the conclusion that the pylons would need to be modified in order to demonstrate flutter suppression. The results of a ground vibration test performed on the 1/2 scale F-16 flutter model and a wind tunnel test with this model and a model Decoupler Pylon are given.					
17. Key Words (Suggested by Author(s)) Flutter Flutter Suppression Decoupler Pylon Wing-Store Flutter Aeroelasticity			18. Distribution Statement  		
19. Security Classif. (of this report) Unclassified		20. Security Classif. (of this page) Unclassified		21. No. of Pages 70	
22. Price					